

# Deep inelastic scattering: The early years\*

Richard E. Taylor

Stanford Linear Accelerator Center, Stanford University, Stanford, California 94309

## FOREWORD

Soon after the 1990 Nobel Prize in Physics was announced, Henry Kendall, Jerry Friedman and I agreed that we would each describe a part of the deep inelastic experiments in our Nobel lectures. The division we agreed upon was roughly chronological. I would cover the early times, describing some of the work that led to the establishment of the Stanford Linear Accelerator Center where the experiments were performed, followed by a brief account of the construction of the experimental apparatus used in the experiments and the commissioning of the spectrometer facility in early elastic scattering experiments at the Center.

In a second paper, Professor Kendall was to describe the inelastic experiments and the important observation of scale invariance which was found in the early electron-proton data.

In a final paper, Professor Friedman would describe some of the later experiments at SLAC along with experiments performed by others using muon and neutrino beams, and how these experiments, along with advances in theory, led to widespread acceptance of the quark model as the best description of the structure of the nucleon.

This paper is, therefore, part of a set and should be read in conjunction with the lectures of H. W. Kendall (1991) and J. I. Friedman (1991).

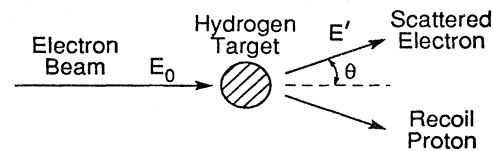
There were many individuals who made essential contributions to this work. Our acknowledgments to a number of them are combined in a fourth "article" (Friedman, Kendall, and Taylor, 1991), which follows the three lectures.

Forty years of electron scattering experiments have had a significant impact on the understanding of the basic components of matter. Progress in experimental high-energy physics is often directly coupled to improvements in accelerator technology and experimental apparatus. The electron scattering experiments, including the deep inelastic experiments cited this year by the Royal Swedish Academy of Sciences, provide examples of this sort of progress. Experiments made possible by increasing electron energy and intensity, along with increasingly sophisticated detectors, have continued to shed light on the structure of nuclei and nucleons over the years. Much additional information has come from

experiments using secondary beams of muons and neutrinos from proton accelerators.

Scattering experiments can trace their roots back to the  $\alpha$ -particle experiments (Geiger and Marsden, 1909) in Rutherford's laboratory which led to the hypothesis of the nuclear atom (Rutherford, 1911). The  $\alpha$  sources used at this time emitted electrons as well as  $\alpha$  particles, but the electron momentum was too small to penetrate beyond the electron cloud of the target atoms, and electron scattering was just an annoying background in those experiments.

Following the landmark experiments of Franck and Hertz (1914) on the interaction of electrons with the atoms of various gases, electron scattering was used extensively to investigate the electronic configurations of atoms. Later, after higher-energy electrons became available from accelerators, interest in their use as probes of the nucleus increased. Rose (1948) gave the first modern treatment of the subject in 1948, followed by Schiff (1949), who was exploring possible experiments for the new electron linear accelerator at Stanford. Schiff stressed the importance of  $e$ - $p$  measurements which could probe the structure of the proton itself using the known electromagnetic interaction. Soon after, Rosenbluth (1950) calculated the probability that an electron of energy  $E_0$  will scatter through an angle  $\theta$  in an elastic collision with a proton—corresponding to the following idealized experimental setup:



The energy  $E'$  of the scattered electron is *less* than the incident energy  $E_0$ , because energy is transferred to the recoil proton (of mass  $M$ ):

$$E' = \frac{E_0}{1 + \frac{2E_0}{M} \sin^2 \theta / 2}.$$

The square of the four-momentum transfer,  $Q^2$ , is a measure of the ability to probe structure in the proton. The uncertainty principle limits the spatial definition of the scattering process to  $\sim \hbar/Q$ ; so  $Q^2$ , and therefore  $E_0$ , must be large in order to resolve small structures.

$$Q^2 = 4E_0 E' \sin^2 \theta / 2.$$

When only the scattered electron is detected, the elastic

\*This lecture was delivered 8 December 1990, on the occasion of the presentation of the 1990 Nobel Prize in Physics.

differential cross section,  $d\sigma/d\Omega$ , obtained by Rosenbluth, is a simple expression, quite similar to the original Rutherford scattering formula:

$$\frac{d\sigma}{d\Omega} = \frac{\alpha^2}{4E_0^2 \sin^4\theta/2} \cos^2(\theta/2) \frac{E'}{E_0} \times \left[ \frac{G_E^2 + \tau G_M^2}{1 + \tau} + 2\tau G_M^2 \tan^2\theta/2 \right],$$

where

$$\tau = Q^2/4M^2.$$

$G_E$  and  $G_M$  are form factors describing the distributions of charge and magnetic moment, respectively. They are functions of only the momentum transfer,  $Q^2$ ,

$$G_E = G_E(Q^2), \quad G_M = G_M(Q^2),$$

$$G_E(0) = 1, \quad G_M(0) = \mu_p,$$

where  $\mu_p$  is the magnetic moment of the proton (in units of  $\hbar$ ). If the charge and magnetic moment distributions are small compared with  $\hbar/Q$ , then  $G_E$  and  $G_M$  will not vary as  $Q^2$  changes; but if the size of those distributions is comparable with  $\hbar/Q$ , then the  $G$ 's will decrease with increasing  $Q^2$ .

Hanson, Lyman, and Scott (Lyman *et al.* (1951) were the first to observe elastic electron scattering from a nucleus using a 15.7 MeV external beam from the 22 MeV betatron at Illinois. They were studying the scattering of electrons by electrons and observed two peaks in the energy spectrum of the scattered electrons (Fig. 1).

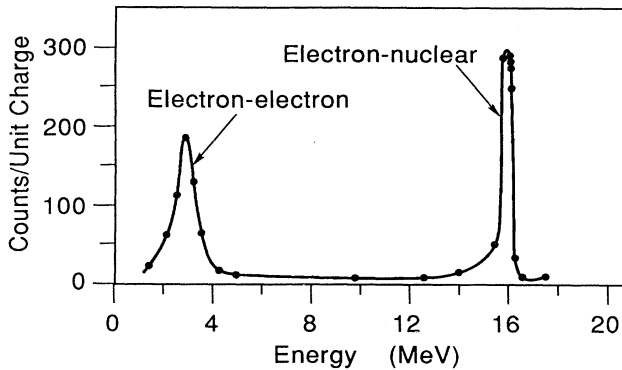


FIG. 1. First observation of elastic electron scattering from a nucleus, using 15.7 MeV electrons from the Illinois betatron, scattered at  $10^\circ$ .

In 1953, the commissioning of the first half of the new Mark III linac in the High Energy Physics Laboratory (HEPL) at Stanford provided an external electron beam of unprecedented intensity at energies up to 225 MeV. Complementing this advance in accelerator technology, Hofstadter and his collaborators constructed a quasi-permanent scattering facility (Fig. 2) based on a  $180^\circ$  magnetic spectrometer (radius of bending = 18 inches). The spectrometer could be rotated about the target to measure different scattering angles, and the excitation of the magnet could be varied to change the energy of the electrons detected. This apparatus was used for a series of experiments with only minor modifications.

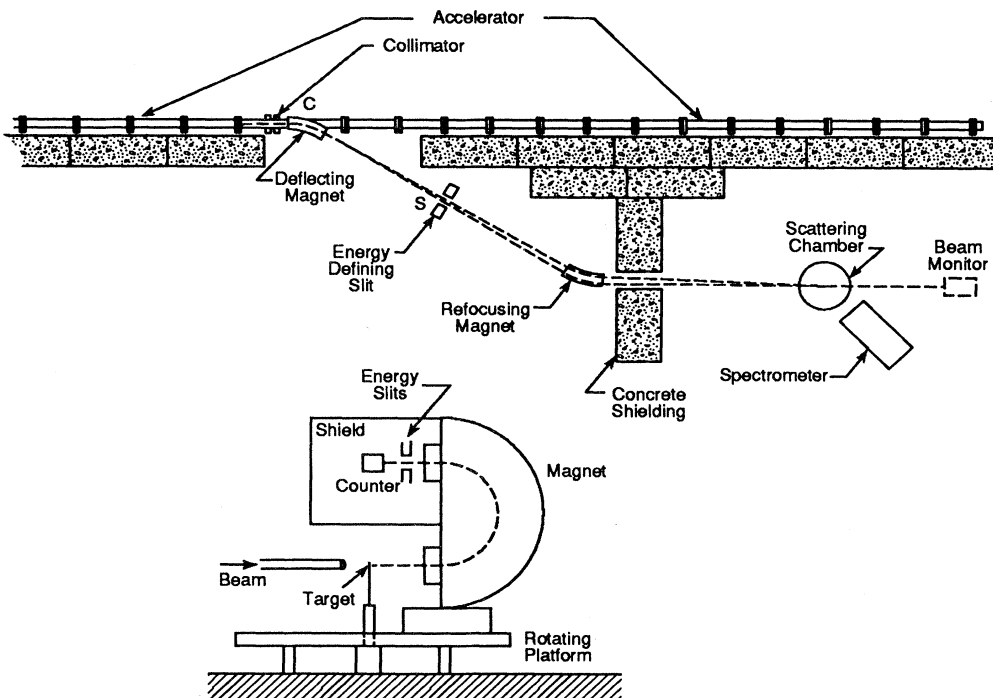


FIG. 2. Schematic of the electron scattering facility located at the halfway point of the Mark III linear accelerator at the High Energy Physics Laboratory at Stanford. The central orbit in the spectrometer has a radius of 18 inches.

Nuclear scattering was easy to observe with this apparatus. At small angles, the “elastic peak” was the most prominent feature of the energy spectrum of the scattered electrons, although scattering with transitions to excited nuclear states was also evident (Fregeau and Hofstadter, 1955; see also Fig. 3). From the behavior of the elastic scattering cross sections at the various beam energies and various scattering angles, Hofstadter and his collaborators were able to measure the size and some simple shape parameters for many nuclides.

In 1953, this facility furnished the first evidence of elastic scattering from the proton, using a polyethylene target (Hofstadter, Fechter, and McIntyre, 1953) as shown in Fig. 4. A hydrogen gas target was then constructed in order to reduce the backgrounds under the elastic peak and in 1955, Hofstadter and McAllister (1955) presented data showing that the form factors in the Rosenbluth cross section were less than unity (Fig. 5)—and were decreasing with increasing momentum transfer. They gave an estimate of  $(0.7 \pm 0.2) \times 10^{-13}$  cm for the size of the proton.

In 1955, new end station facilities at HEPL were commissioned, doubling the energy available for scattering experiments. Beams from the full length of the linac were available in the new area, reaching energies of 550 MeV (Fig. 6). A new spectrometer facility was installed by Hofstadter's group with a magnet of twice the bending radius (36 inches) of the spectrometer in use at the halfway station. A liquid hydrogen target was constructed and installed. This equipment was a considerable improvement (Fig. 7), and a large effort was focused on scattering from hydrogen (Hofstadter, 1956<sup>1</sup>; see also Hofstadter and McAllister, 1955). A graph of the measured form factors is shown in Fig. 8, which shows data for various values of  $Q^2$  compared with a model proton with a “size” of  $0.8 \times 10^{-13}$  cm.

These experiments mark the beginning of the search for substructure in the proton. They showed persuasively that the proton was not a point, but an extended structure. This fundamental discovery was rapidly accepted by the physics community. It was generally assumed that there was a connection between spatial extent and structure, although I don't think anyone was seriously questioning the “elementary” character of the proton at that time. The available electron energies were not yet high enough for the exploration of inelastic scattering from the proton, and only elastic experiments provided clues about proton structure for the next several years.

The new facility was also used to measure scattering from deuterium, in order to extract information about the neutron. The form factor for elastic scattering from the loosely bound deuterium nucleus falls off extremely rapidly with increasing momentum transfer, so the neu-

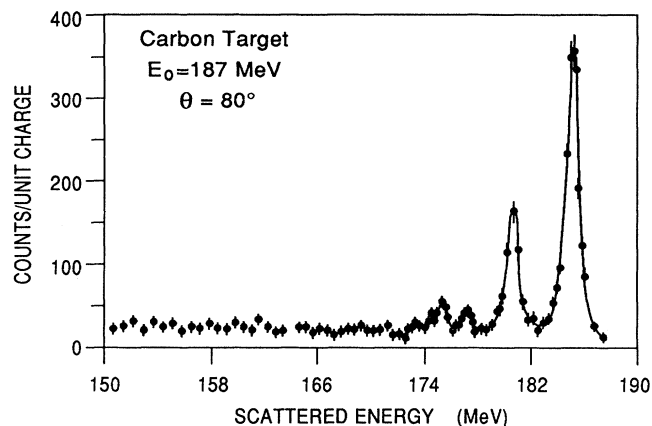


FIG. 3. Energy spectrum of 187 MeV electrons scattered through  $80^\circ$  by a carbon target, using the apparatus in Fig. 2.

tron was studied via quasi-elastic scattering—scattering from either the proton or the neutron, which together form the deuterium nucleus. The quasi-elastic scattering reaches a maximum near the location of the peak for electron-proton scattering, since the scattering takes place off a single nucleon and the recoil energy is largely determined by the mass of that nucleon (Fig. 9). One also observes the effects of the motion of the nucleons in deuterons, and one result is a measurement of the nucleon's momentum distribution in the deuterium nucleus.

The great success of the scattering program at HEPL had three consequences: Scattering experiments became

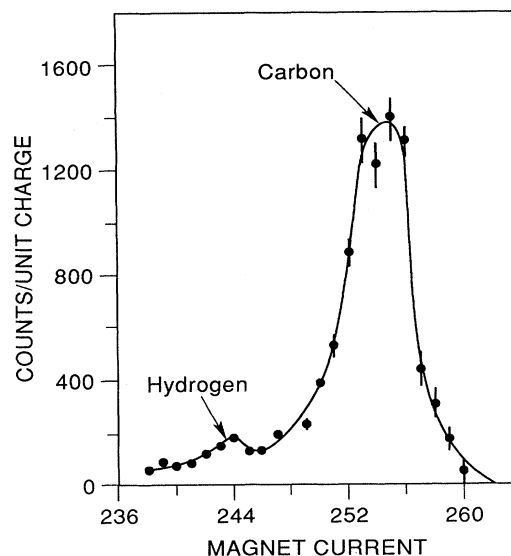


FIG. 4. Spectrum of scattered electrons from a  $\text{CH}_2$  target showing evidence of electron-proton scattering, circa 1954.

<sup>1</sup>This article summarizes the work at HEPL up to 1956 and contains a fairly complete set of references to the early work in the field.

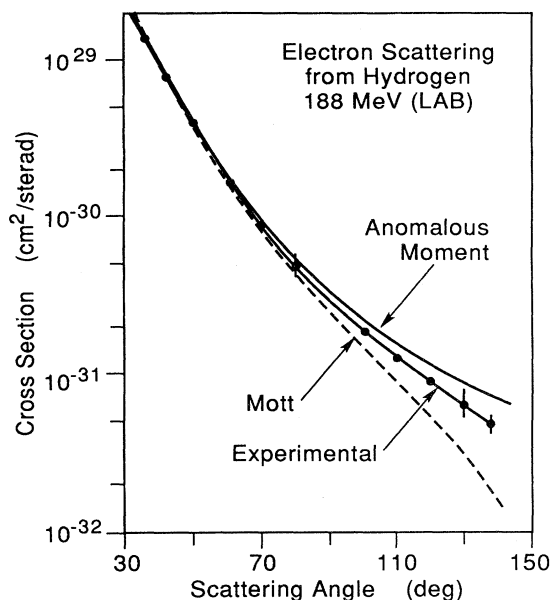


FIG. 5. Elastic electron scattering cross sections from hydrogen compared with the Mott scattering formula (electrons scattered from a particle with unit charge and no magnetic moment) and with the Rosenbluth cross section for a point proton with an anomalous magnetic moment. The data falls between the curves, showing that magnetic scattering is occurring but also indicating that the scattering is less than would be expected from a point proton.

more popular at existing electron synchrotrons; new synchrotrons were planned for higher energies; and discussions began at Stanford about a much larger linear accelerator—two miles long and powered by one thousand klystrons!

After more than a year of discussions and calculations, the physicists and engineers of the High Energy Physics Laboratory prepared the first proposal for a two-mile linear accelerator to be built at Stanford (Ginzton *et al.*, 1957). E. L. Ginzton, W. K. H. Panofsky, and R. B. Neal directed the design effort, and Panofsky and Neal went on to direct the construction of what came to be called the Stanford Linear Accelerator Center (SLAC)—surely one of the great engineering achievements of the early 1960s (Neal, 1968). The new machine was a bold extrapolation of existing techniques. The design was conservative in the sense that working prototypes of all the machine components were in hand, but a formidable challenge because of the increase in scale.

The investigation of the structure of the proton and neutron was a major objective of the new machine. The 20 GeV energy of the accelerator made both elastic and inelastic scattering experiments possible in a new range of values of  $Q^2$ , and presented our collaboration with a golden opportunity to pursue the studies of nucleon structure.

When it was proposed, the two-mile linac was the largest and most expensive project ever in high-energy physics. Up until that time the field had been dominated by proton accelerators, and electron machines had been relatively small and few in number. Electrons were catching up, and, in parallel with SLAC, two large electron synchrotrons were proposed and built—the Cambridge Electron Accelerator (CEA) and the Deutsches Elektronen Synchrotron (DESY) in Hamburg, with peak energies of 5 and 6 GeV, respectively. The establishment of SLAC in 1960 would eventually bring electron physics into direct competition with the largest proton accelerators of the time, the Brookhaven AGS and the CERN

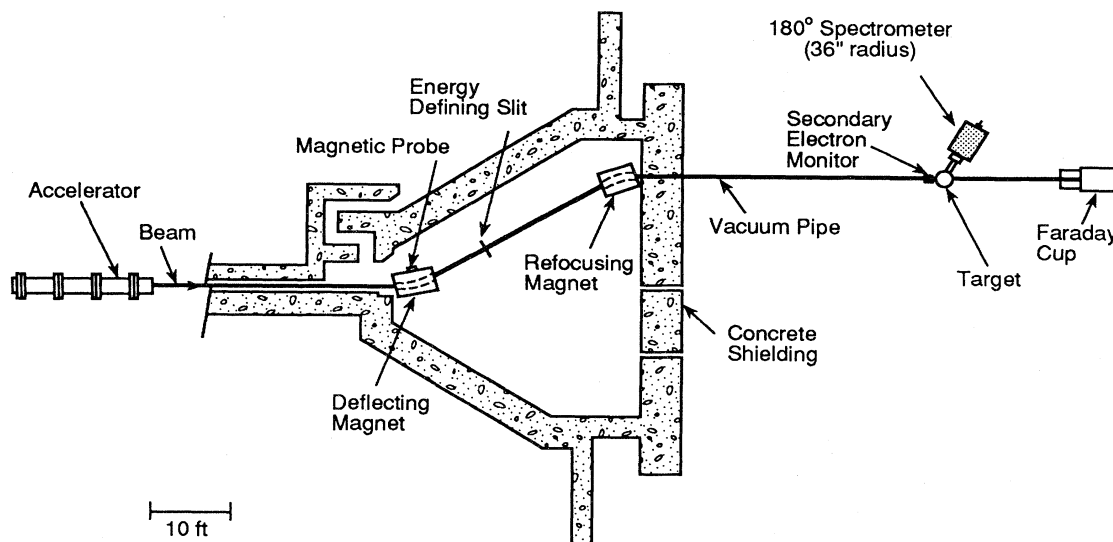


FIG. 6. Layout of the beam line and the 36-inch spectrometer in the End Station of the High Energy Physics Laboratory. This facility was used for electron scattering experiments for more than a decade by R. Hofstadter and his collaborators. (A 72-inch spectrometer was added in 1960 to analyze scattered electrons to an energy of 1000 MeV.)

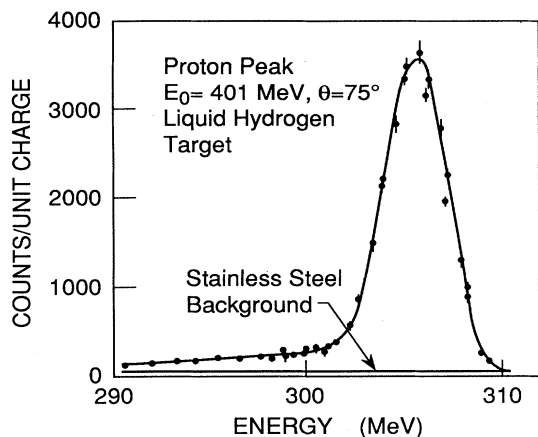


FIG. 7. Electron-proton scattering energy spectrum taken using the facility in Fig. 6 and a liquid hydrogen target. The stainless-steel container for the liquid hydrogen contributes very little background. The radiative tail of the elastic peak is clearly evident on the low-energy side of the peak.

PS, both of which were already under construction in the late 1950s. The new electron accelerators would make available many opportunities for physicists.

The new linear accelerator consisted of two miles of accelerating waveguide, mounted in a tunnel buried 25

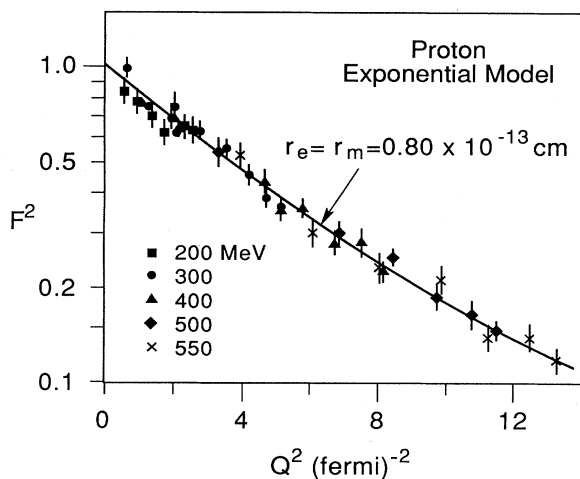


FIG. 8. The proton form factor for various energies and momentum transfers as measured in early experiments using the 36-inch spectrometer facility at HEPL. The value of  $F^2$  was calculated from the original Rosenbluth formula which defined form factors  $F_1(Q^2)$  and  $F_2(Q^2)$ .  $F_1$  corresponds to the form factor for a Dirac (spin- $\frac{1}{2}$ ) proton, and  $F_2$  to the form factor for the anomalous magnetic moment. In the analysis of the data it was assumed that  $F_1 = F_2$ . At higher values of  $Q^2$  it became evident that  $F_1 \neq F_2$ , but rather that  $G_E = G_M/\mu_p$  for the proton, and the use of the  $G$ 's then became universal. ( $G_M = F_1 + KF_2$  and  $G_E \approx F_1$  for small values of  $Q^2$ .) The curve shown in the figure was based on a model assuming exponentially falling distributions of charge and magnetic moment, each with a root-mean-square radius of  $0.8 \times 10^{-13}$  cm [1 fermi =  $10^{-13}$  cm,  $1 \text{ (fermi)}^{-2} = 0.0388 \text{ GeV}^2$ ].

feet underground. In the initial phase, the waveguide was powered by two hundred and forty 20–30 MW klystrons housed in a building at ground level. The accelerator was sited in the hills behind Stanford on University land and was probably the last of the university-based high-energy physics accelerators in the U.S. (Figs. 10 and 11).

The design parameters of the new machine—20 GeV in energy and average currents in the neighborhood of  $100 \mu\text{A}$ —presented many new problems for experimenters. Two experimental areas (called End Stations in Fig. 12) were developed initially—one heavily shielded area, where secondary beams of hadrons and muons could be brought out to various detectors, and a second area for electron and photon beam experiments. The “beam switchyard” connected each area to the accelerator with a magnetic beam transport system, which defined the momentum spread of each beam to better than 0.2%, was achromatic and isochronous (in order to preserve the RF time structure of the beam). The transport systems were fed by a system of pulsed magnets, so that a given accelerator pulse could be directed into either of the two experimental areas. Unavoidable beam losses in the system would lead to high levels of radioactivity and to challenging thermal design problems at the expected levels of beam currents. The design of this switchyard area was fairly well fixed by the end of 1963, along with the specifications for the heavily shielded end station buildings (see Neal, 1968).

The experimental area which was to be devoted to

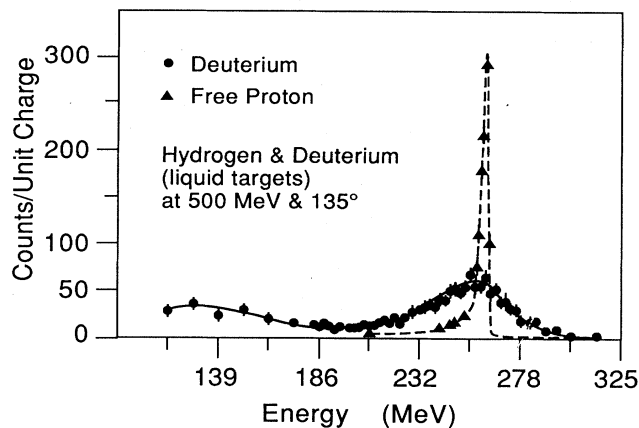


FIG. 9. A comparison of the scattering of electrons from the proton and the quasi-elastic scattering from the individual nucleons in deuterium. The elastic scattering from the deuterium nucleus would occur at an energy above the highest energy shown on the graph and would be negligible in comparison with the cross sections illustrated here. The quasi-elastic scattering from either the proton or the neutron in deuterium is spread out over a wider range of energies than the scattering from the free proton because of the momentum spread of the nucleons in the deuterium nucleus.

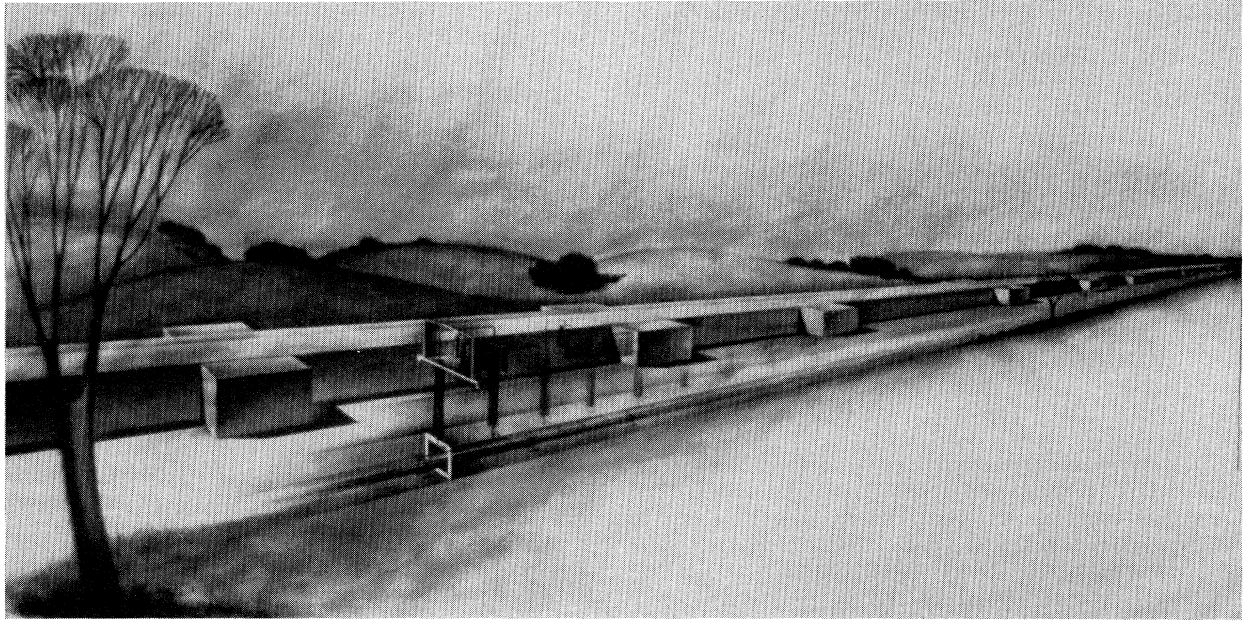


FIG. 10. Cutaway illustration of the two-mile Stanford Linear Accelerator, showing the accelerator waveguide buried 25 feet below the surface and the klystron gallery at ground level. Each klystron feeds 40 feet of accelerator waveguide through penetrations connecting the accelerator housing with the klystron gallery.

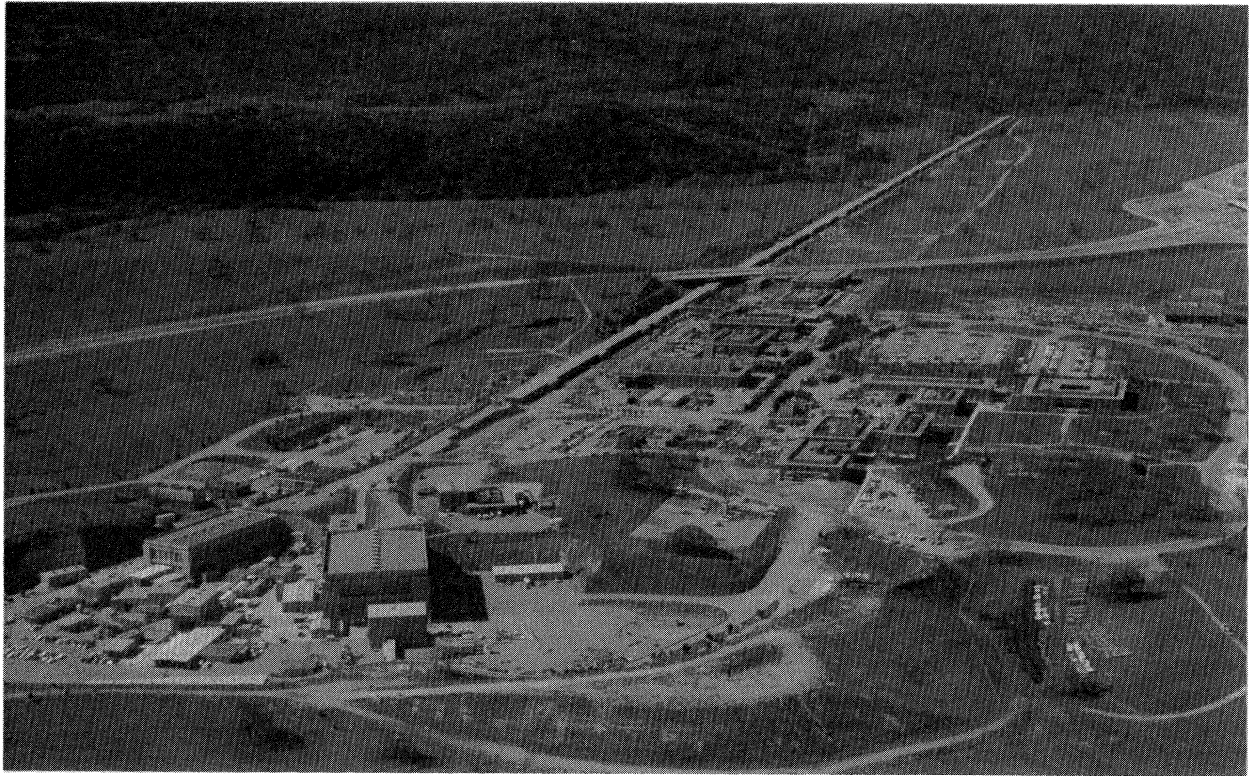


FIG. 11. Aerial view of the SLAC site. On the left are the experimental areas fed by beam lines from the accelerator. On the right is the campus area where offices, laboratories, and shops are located. The scattering experiments were performed in the large shielded building just to the left of center near the bottom of the picture. The structure crossing the accelerator is a superhighway which was under construction at the time this picture was taken.

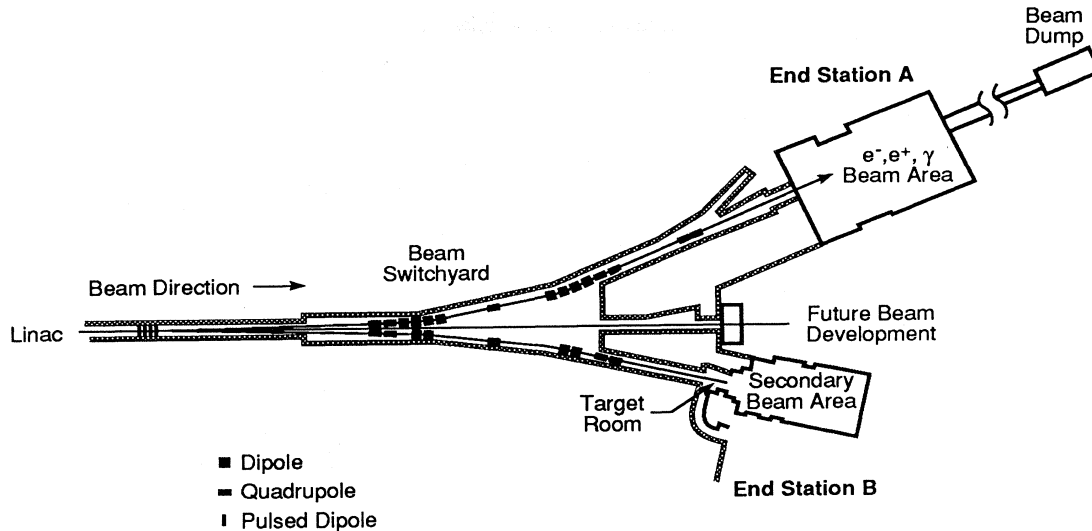


FIG. 12. Layout of the SLAC experimental areas and the beam switchyard.

electron scattering and photoproduction experiments using the primary beam had to satisfy the experimental needs of several groups of experimenters. The challenge was to build apparatus which would allow rapid and efficient data collection in the new energy region which was being made available. The operating costs of the new accelerator (not to mention the depreciation on the capital costs of over 100 million dollars) would be many thousands of dollars per day, so it was important to balance costs in such a way that the experiments would give good value—a spectrometer with small solid angle would be cheaper, but might take much longer to make a given measurement. The major costs in this area would be for large magnetic spectrometers and shielding, and so some of the smaller components could be developed to a much more sophisticated level than had been possible at the smaller laboratories, while still adding only a small percentage to the overall costs.

Although half a decade had passed since the original proposal for SLAC, the basic physics aims remained much the same. The most effective technique still appeared to be the detection of a single particle from a given interaction. [The duty factor (i.e., the percentage of on time) was low for the linac—the klystrons were pulsed for approximately two microseconds, at a rate of 360 times per second. This results in high instantaneous rates during the short pulses and made coincidence experiments difficult.] The overall experimental design required instruments which would determine the energy and angle of a particle coming from a target placed in the beam of electrons. Magnetic spectrometers were still the most effective way to accomplish this, but they would be large and cumbersome devices at these energies.

The resolution in energy,  $\Delta E$ , had to be much better than  $m_\pi/E_{\max} \sim 0.7\%$  in order to separate reactions that differed in the number of pions emitted. Since the energy of particles from a given reaction is a very steep function

of angle, it was also necessary to measure the angle of scattering to high accuracy ( $\sim 0.15$  milliradians). Practical spectrometers have angular acceptances much greater than the required resolution in angle; so the optics and the detectors had to be arranged in such a way that the true angle of scattering was determined along with the energy.

There were many discussions about the most effective design for the facilities. Records are sparse, but there are indications of frank and earnest discussions. There was a suggestion that a single 2 GeV spectrometer could cover most of the interesting electron scattering experiments, while others were suggesting that a complex system with a high-energy forward spectrometer combined with a huge solenoidal detector in the backward direction was the right way to go.

In the spring of 1964, I found myself gradually being elected to a position of responsibility for the design and engineering of the facilities in End Station A (as the larger of the two experimental areas was called). This was not an enviable position, since there was little agreement about what should be done and most of the people involved clearly outranked me.

The subgroup interested in electron scattering experiments was pretty well convinced that a spectrometer of 8–10 GeV maximum energy with a solid angle  $\gtrsim 1$  milliradian would be capable of an extensive program of scattering measurements. By bending in the vertical plane, measurements of scattering angle and momentum could be separated at the location of the detectors. Preliminary designs for such a device had been proposed and had already influenced the layout of the end station, which by this time was in an advanced state of design. The spectrometer incorporated a vertical bend of  $\sim 30^\circ$ , with focusing provided by separate quadrupoles preceding and following the bend (Fig. 13, elevation). The magnetic design of the spectrometer involved a lot of compu-

tation, but proceeded smoothly. After taking practical and financial constraints into account, the top momentum was fixed at 8 GeV and the solid angle at 1.0 milliradians.

In order to cover a range of scattering angles it was our intention to build the spectrometer so that it could be rotated around the target from an external control room (Fig. 13, plan). We needed frames which would hold

hundreds of tons of magnets and counters in precise alignment while they were moved about the end station.

It was about this time that we began to assemble a team of engineers and draftsmen to translate the requirements into designs for working hardware. The group began the detailed design of the 8 GeV spectrometer components, while the debate continued about the rest of the complex.

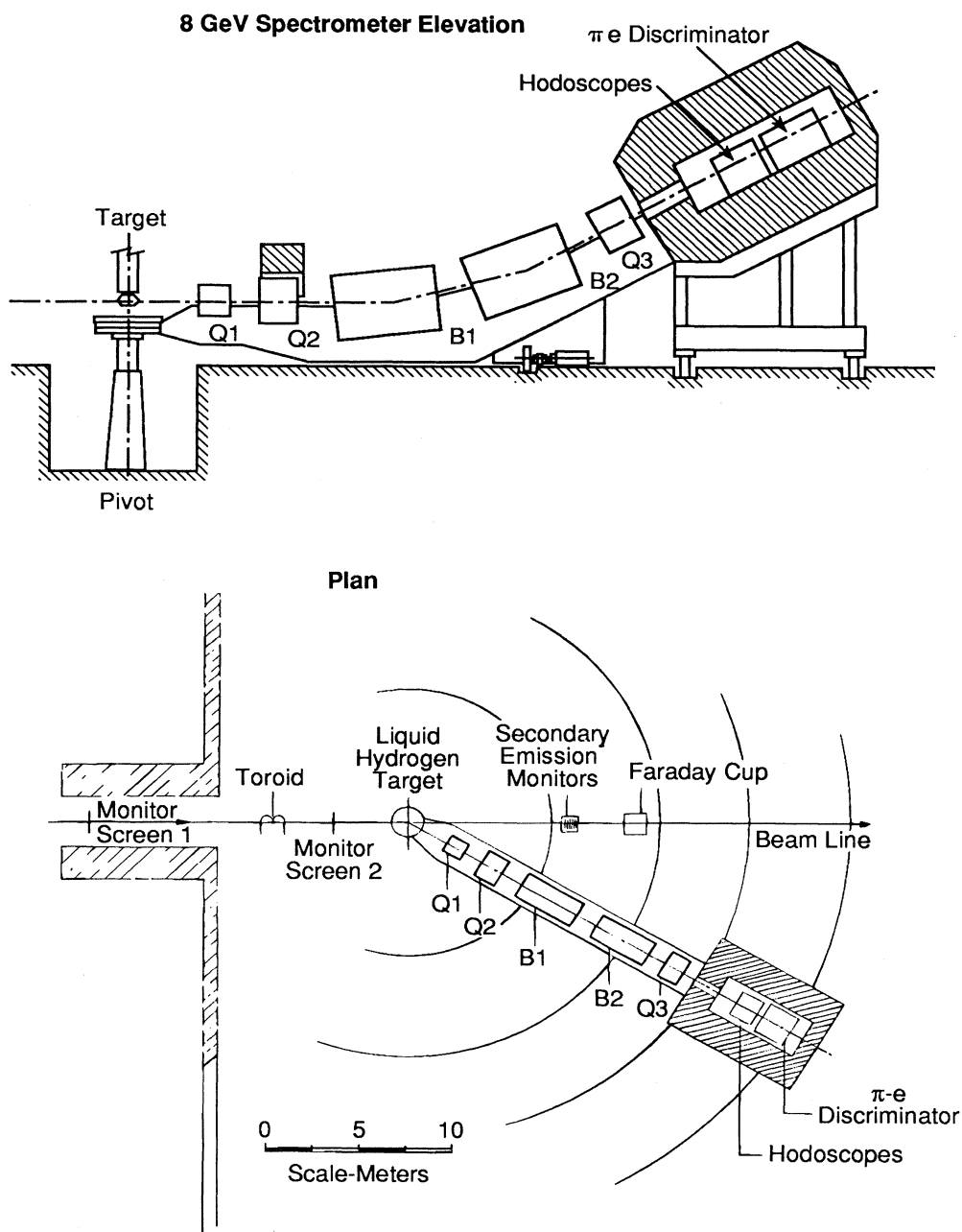


FIG. 13. Schematic drawings of the 8 GeV spectrometer. Five magnets [two bending magnets ( $B$ ) and three quadrupoles ( $Q$ )] direct scattered particles into the detectors which are mounted in a heavily shielded enclosure. The whole assembly rides on the rails and can be pivoted about the target to change the angle of scattering of the detected electrons.



By the middle of 1964 the utility of a forward-angle spectrometer which would analyze particles with a maximum momentum of 20 GeV was no longer questioned. Successful photoproduction experiments were being carried out at energies up to 5 GeV at the CEA electron synchrotron, and extending the energy of these measurements would obviously be a productive program for SLAC. Also, if the electric form factor of the proton,  $G_E$ , were to be measured, small-angle scattering experiments would be required.

Scaling up the 8 GeV spectrometer to 20 GeV (and keeping the resolution at 0.1%) would have required very large vertical displacements. Some attempts were made to design a big pit in the end station to accommodate such a system which would bend downward, but it looked very awkward from a mechanical viewpoint. An ingenious solution was proposed by Panofsky and Coward, in which horizontal bending could be used while preserving orthogonal momentum and angle measurements at the focus. This proposal seemed complicated to me, and I resisted adopting the design. Finally, I was rescued by K. Brown's calculation of aberrations in this device, which he found to be unacceptably large. Shortly thereafter, Brown and Richter proposed a relatively simple spectrometer with a central crossover which allowed vertical bending, but kept the vertical height within bounds. A relatively simple system of sextupoles was required to correct aberrations in the system. Once proposed, this design was accepted by all, and final layout of the spectrometers in the end station was soon accomplished (Fig. 14).

The two large groups at SLAC were not very interested in measurements in the backward direction at the time. But D. Ritson of the Stanford Physics Department saw an opportunity to continue his HEPL program of photoproduction measurements at higher energies, and

proposed the construction of a 1.5 GeV, 90° spectrometer at large angles, a proposal which was accepted by the laboratory after a short delay, and the spectrometer was added to the facility.

With the magnetic design of the two large spectrometers fixed, design and construction of the facility began in earnest. The building of the facility was a joint effort of the SLAC-MIT-CIT group, the SLAC photoproduction group under B. Richter, and the Stanford group interested in the 1.6 GeV spectrometer led by D. Ritson. The facility consisted of several parts.

The 8 GeV spectrometer used five magnetic elements—three quadrupoles and two bending magnets (Fig. 15). It had point-to-point focusing in the vertical plane (the plane in which momentum is dispersed). A detector hodoscope in the  $p$  focal plane defined the differential momentum,  $\Delta p$ . In the horizontal plane (scattering plane), the spectrometer gave parallel-to-point focusing, allowing the use of a long target. A second hodoscope in the  $\theta$  focal plane determined the scattering angle. The  $p$  and  $\theta$  focal planes were located close to each other, but were not coincident.

The 20 GeV spectrometer used eleven magnetic elements—four bending magnets, four quadrupoles, and three sextupoles—to produce very similar conditions at the  $p$  and  $\theta$  focal planes (Fig. 16). An added feature was the extra  $p$  focus in the middle of the magnetic system. A slit at this point could be used to control the  $\Delta p/p$  band-pass of the instrument. A system of counters similar to those in the 8 GeV spectrometer was mounted in the shielding hut.

The 1.6 GeV spectrometer had only a single magnetic element (Fig. 17). Focusing was achieved by rotation of the pole tips out of the normal to the central orbit. Some sextupole fields were built into the pole faces to control aberrations.

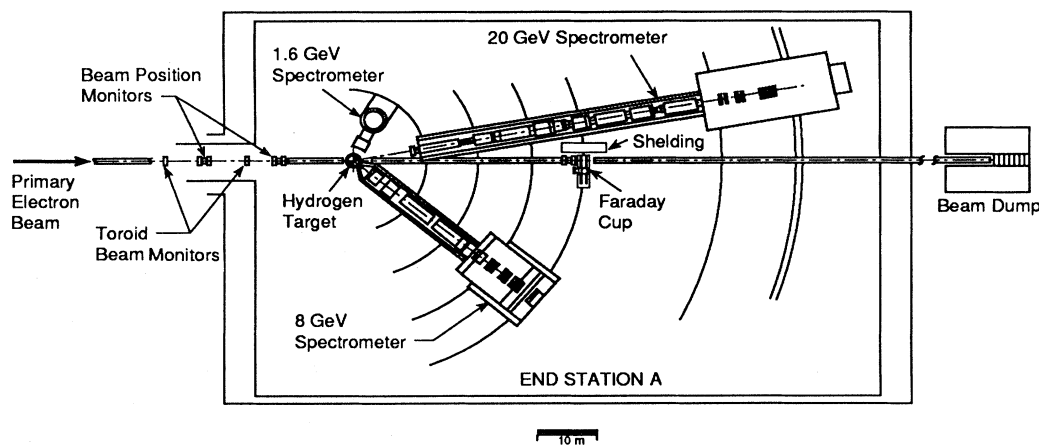


FIG. 14. Layout of spectrometers in End Station A. All three spectrometers can be rotated about the pivot. The 20 GeV spectrometer can be operated from about  $1\frac{1}{2}^\circ$  to  $25^\circ$ , the 8 GeV from about  $12^\circ$  to over  $90^\circ$ . The 1.6 GeV spectrometer coverage is from  $\sim 50^\circ$ – $150^\circ$ .

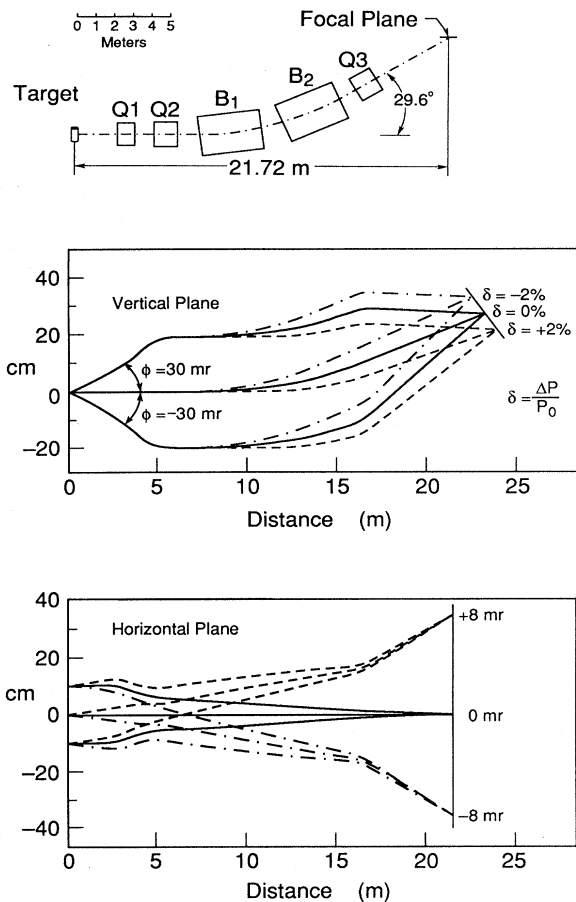


FIG. 15. The magnet layout and optics of the 8 GeV spectrometer. The arrangement of magnets is shown at the top of the figure. In the vertical plane the focusing is “point to point” and momenta are dispersed along the focal plane. In the horizontal, the focusing is parallel to point and angles are dispersed along the  $\theta$  focal plane (mr=milli-radian).

The liquid hydrogen targets for the facility were of the condensation type. In these devices a separate target cell was in thermal contact with a reservoir of liquid hydrogen at atmospheric pressure. Gaseous hydrogen (or deuterium) introduced into the target cell at greater than atmospheric pressure would condense to the liquid phase.

The first target built for the facility was very simple in concept and used convection in the target cell to transfer the heat generated by the passage of the beam to the reservoir. It turned out that this mechanism was not effective at high beam power levels, and that, as a result, intense beams caused fluctuations in the liquid density. Targets were then built that used forced circulation by a fan to keep the liquid in the target cell in closer thermal contact with the reservoir. Schematics of both targets are shown in Fig. 18. (Even the circulating targets had some problems at very high beam currents.)

The accuracy to which cross sections can be measured is directly related to the accuracy with which the incident-beam intensity can be measured. The primary standard for the early experiments was a Faraday cup [Fig. 19(a)] in which 20 GeV electrons were stopped and the resulting charge measured with an accurate current integrator. The Faraday cup could not be used with the full beam power of the linac because of thermal limitations, but it was used to calibrate other monitors at low repetition rates.

A new toroid monitor was specifically developed for the End Station A experiments. The principle of operation is illustrated in Fig. 19(b). The beam acted as the primary winding of a toroidal transformer. Passage of a beam pulse through the toroid set up an oscillation, and the amplitude of that oscillation was sampled after a certain fixed interval. The sampling and subsequent readout of the signal determined the final accuracy of the monitor. The readout was carefully engineered by the SLAC electronics group, and as experience with this device increased, it became the absolute standard for beam

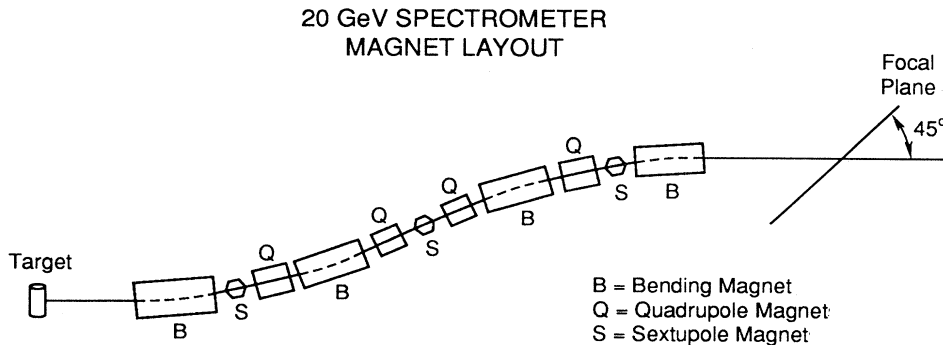


FIG. 16. Magnetic system for the 20 GeV spectrometer. With a momentum focus at the central sextupole, the final two bending magnets add to the momentum dispersion, even though the direction of bending is opposite to that in the first two bending magnets. The three sextupoles are used to adjust the angle of the focal plane to a convenient value.

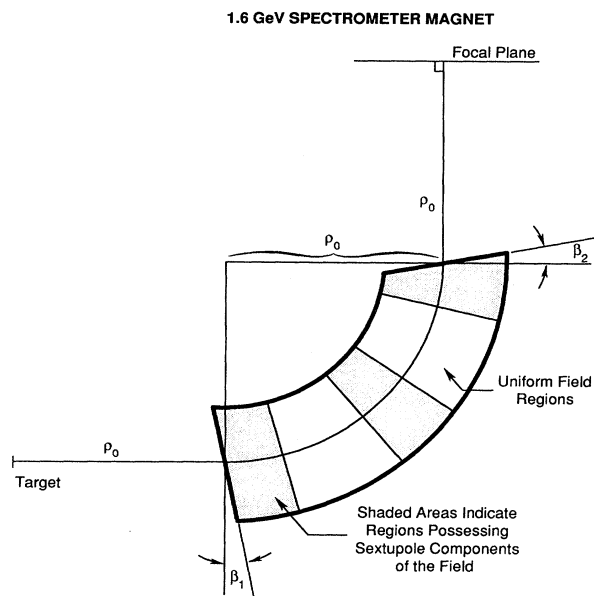


FIG. 17. Schematic of the 1.6 GeV spectrometer. Focusing is achieved by rotated pole tips (angles  $\beta_1$  and  $\beta_2$ ), and sextupoles are built into the pole faces to adjust the focal plane to be at right angles to the central ray.

current measurements, though often cross-checked against the Faraday cup.

In addition to the beam monitors, there were various collimators and screens along the beam line, and a high-power beam dump buried in a hill a hundred meters or so

behind the end station. An impressive cable plant connected the spectrometer detectors to the electronics in the "counting house" high above the end station floor.

I wish I had the skills to recreate for you the three years of intense activity that went into translating the paper plans of 1964 into the instruments which began to do physics in early 1967. The problems in procuring the precision magnets, the construction of the giant frames to hold the magnets and to support the massive shields for the detectors, the laying of the rails to extraordinary tolerances—all these and many other problems were attacked with drive and dedication by the mechanical engineering group. Even the professional crews hired to install large parts of the apparatus became infected with the enthusiasm of the engineers. I lived in mortal fear that a union steward would drop in unannounced and find a millwright (steelworker) building a wooden scaffold, while a carpenter was operating the crane. Figure 20 is a view of the experimental area with the completed 8 and 20 GeV spectrometers in place.

The 8 GeV detectors were designed and built at MIT (Fig. 21). Two large scintillation counters acted as trigger counters, signaling the passage of charged particles through the counter system. Two multi-element scintillation counter hodoscopes (mounted between the trigger counters) defined the position of the track in the horizontal ( $\theta$ ) and vertical ( $p$ ) directions. The hodoscopes each consisted of two layers of overlapping counters, so that each double hit defined the position to half a counter width. The location of the hits together with the angle and energy setting of the spectrometer defined the angle of scattering to  $\pm 0.15$  milliradians and the momentum of

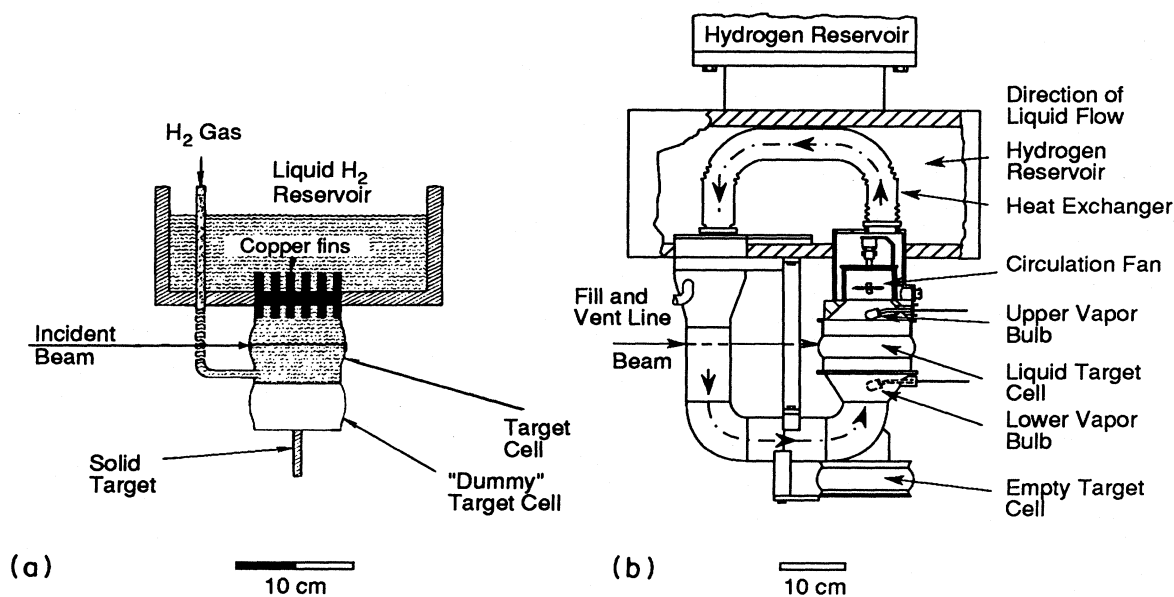


FIG. 18. (a) Schematic of the first condensation hydrogen target built for the End Station A facility. The target could be displaced vertically to put either the dummy target or the solid targets on the beam line. (b) Schematic of a condensation target with forced circulation of the condensed hydrogen. As in (a), the target could be displaced vertically so that other targets could be placed in the beam line.

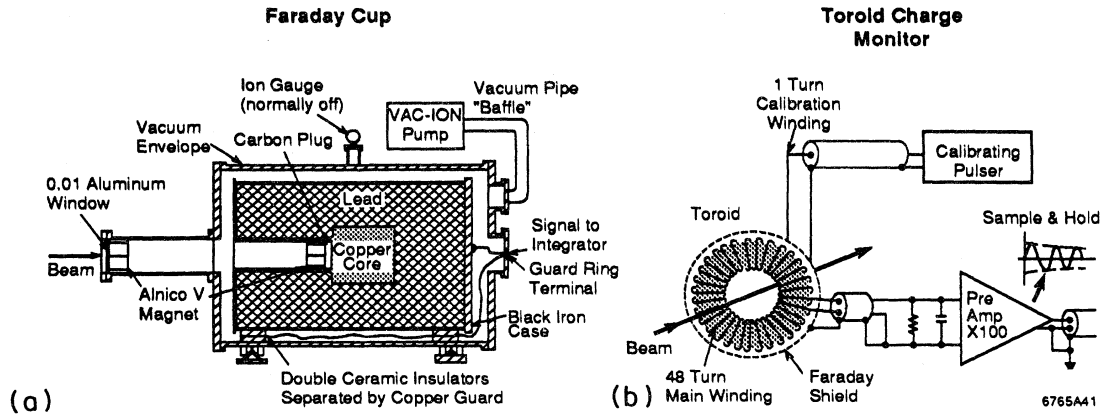


FIG. 19. (a) Drawing of the Faraday cup. The beam was stopped in the carbon-copper core of the cup, and the lead absorbed  $\gamma$  rays created in the shower. The alnico magnets deflected low-energy electrons coming from the window so that they did not reach the cup and those from the core did not escape from it. (b) Schematic of the toroidal transformer monitor. The beam acted as the primary winding of the ferrite core. A beam pulse caused a “ringing” of a damped  $LC$  circuit, the amplitude of which was read out after three quarters of a cycle.

the scattered particle to  $\pm 0.05\%$ . Following the system of hodoscopes was a set of counters used to distinguish electrons from pions. The principal element was a total absorption lead-lucite shower counter. The pulse height threshold was set to be more than 99% efficient for electrons. In the elastic scattering experiments this counter

alone was enough to ensure a pure electron signal, but for inelastic scattering, pion backgrounds increased and the use of the  $dE/dx$  counters was sometimes necessary. These counters measured the energy loss in a scintillator for particles which have passed through one radiation length of lead. Electrons will often shower in the radia-

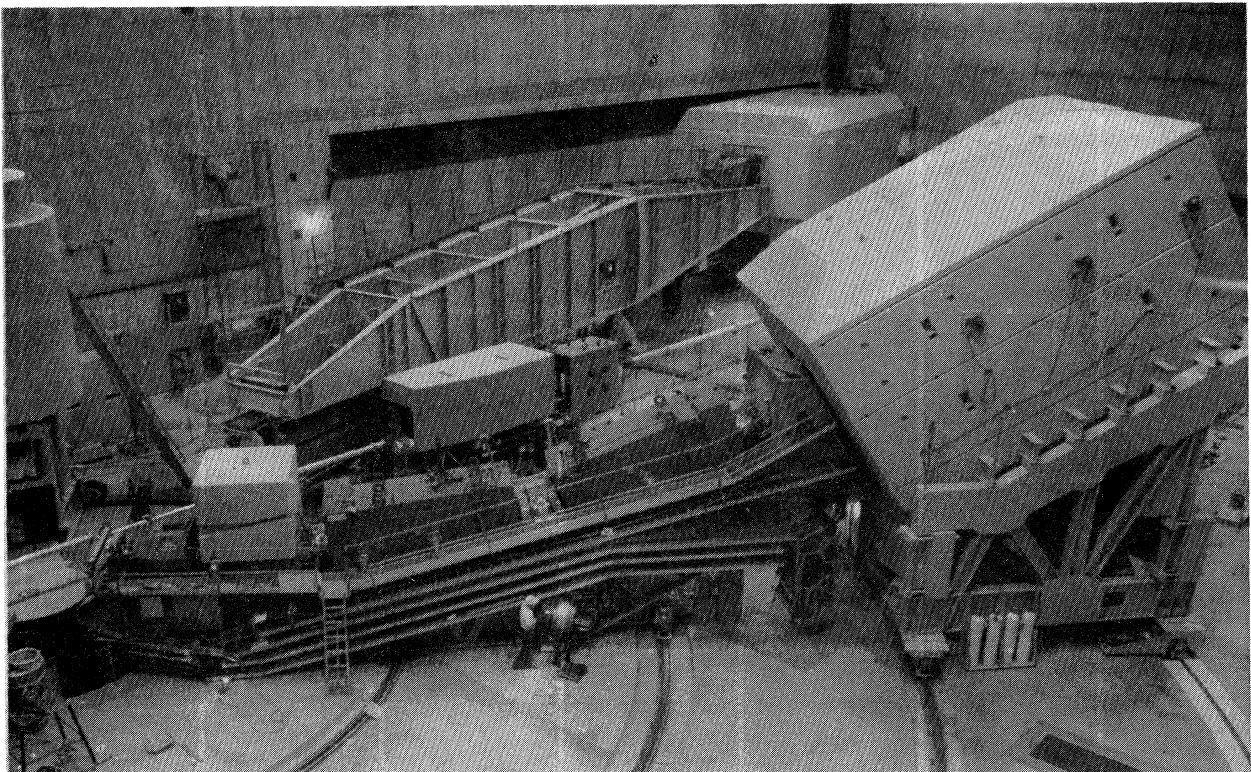


FIG. 20. Photograph of the 8 and 20 GeV spectrometers in End Station A.

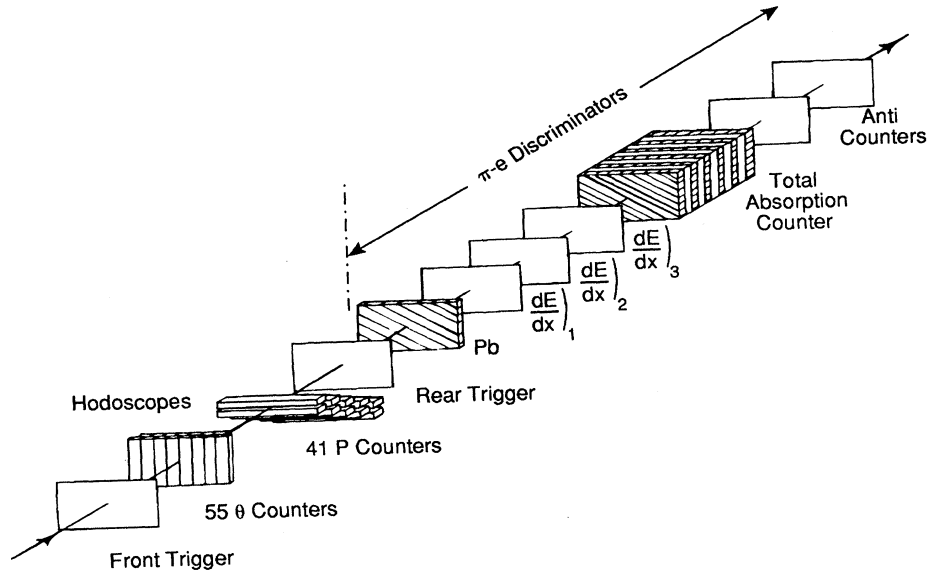


FIG. 21. Schematic drawing of the counter system inside the 8 GeV shielding hut.

tor, giving large pulse height in the counters. In most cases pions will not shower, giving an almost independent indication of their identity. By the time of the first inelastic scattering experiments using the 8 GeV spectrometer, a gas Čerenkov counter had been added in front of

the trigger counter as a further tool for particle discrimination. The  $dE/dx$  system was used only for the lowest secondary energies where the pion-electron ratios were large. The 20 GeV spectrometer's counter system (Fig. 22) was similar to that in the 8 GeV spectrometer, with

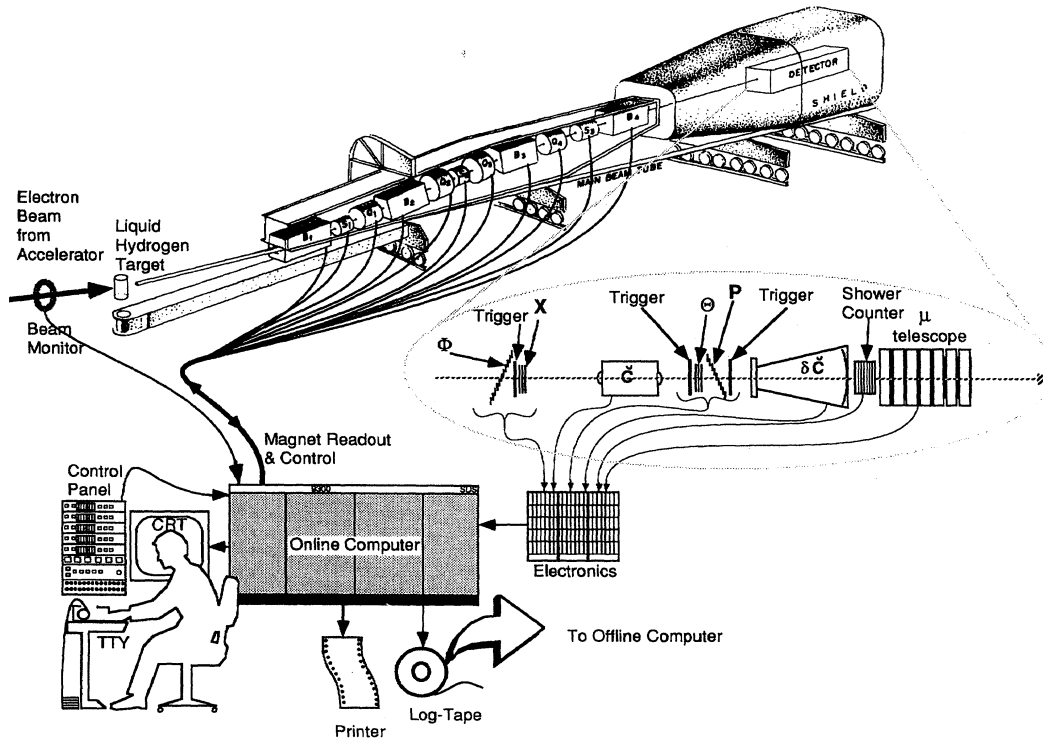


FIG. 22. Schematic of the 20 GeV spectrometer indicating the various computer control and readout functions. Also shown is a schematic of the 20 GeV counter system. Particle identification in the spectrometer was somewhat more complex than for the 8 GeV instrument, partly because of the higher energies involved, but also because it was sometimes desirable to identify  $\pi$  mesons in a large electron background in the 20 GeV spectrometer.

the addition of a differential gas Čerenkov counter and extra sets of hodoscopes which determined the angle of scatter outside the horizontal plane ( $\varphi$  hodoscope) and the position of the scattering center along the beam line ( $x$  hodoscope). The MIT group also took responsibility for much of the counting electronics, photo tube power supplies, etc., and were of great assistance to the electrical engineers in the SLAC group who installed the electronics and interfaced the on-line computer.

One innovation by the collaboration was the extensive use of on-line computation in the experiment. While not the first experiment to be equipped with an on-line computer, the degree of computer control was ambitious for the time. We purchased a fairly powerful mainframe, dedicated to only one experiment at a time. A lot of work was done on both software and hardware, so that the effort to set up and operate a given experiment was greatly reduced. The on-line analysis of a fraction of the increasing data was a powerful way to check on the progress of the experiments (Fig. 22).

In the summer of 1966 there was a call for proposals to use the beam at SLAC. The accelerator was nearing completion, and some early tests of the accelerator with beam were being done with considerable success. Although the initial programs in End Station A were built into the design of the facility, it was now necessary to parcel out beam time and arrange the sequence of experiments for the first year of operation. The Caltech-MIT-SLAC collaboration prepared a proposal that consisted of three parts:

- (a) Elastic electron-proton scattering measurements (8 GeV spectrometer);
- (b) inelastic electron-proton scattering measurements (20 GeV spectrometer);
- (c) comparison of positron and electron scattering cross sections (8 GeV spectrometer).

It is clear from the proposal that the elastic experiment was the focus of interest at this juncture: "We expect that most members of the groups in the collaboration will be involved in the  $e$ - $p$  elastic scattering experiment, and that the other experiments will be done by subgroups."

During the construction of SLAC and the experimental facilities, a lot of progress had been made on the measurements of nucleon form factors at other laboratories. The program at HEPL had continued to produce a great deal of new data using the facilities in the end station of the Mark III accelerator. A new spectrometer with a bending radius of 72 inches had been added to accommodate the increased energy available from the accelerator. Extensive results on both the proton and the deuteron were generated and reported (Buchanan *et al.*, 1965<sup>2</sup>; see also Neal, 1968 and Fig. 23).

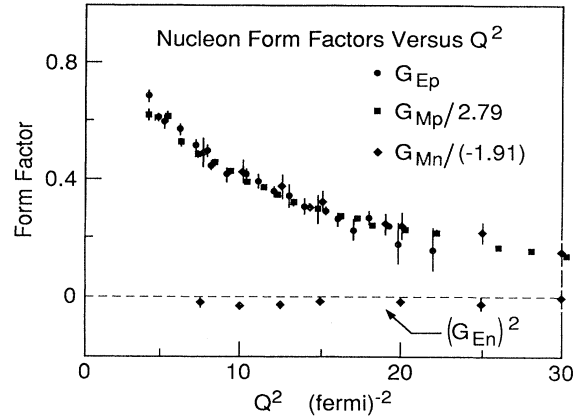


FIG. 23. Summary of results on nuclear form factors presented by the Stanford group at the 1965 international symposium on electron and photon interactions at high energies. (A momentum transfer of 1 GeV<sup>2</sup> is equivalent to 26 fermis<sup>-2</sup>.)

At over 1 GeV, the Cornell electron synchrotron was the highest energy electron machine in the world for a few years in the early 1960s. Experimenters there made a series of measurements on CH<sub>2</sub> targets, using a quadrupole spectrometer of novel design (Wilson *et al.*, 1960; Fig. 24) and a new type of  $\alpha$ -ray monitor (Wilson, 1957). The results from Cornell started a trend toward the use of the electric and magnetic form factors ( $G_E$  and  $G_M$ ; see Berkelman *et al.*, 1963), rather than one form factor for a spin-1/2 (Dirac) proton and a second for the "anomalous" magnetic moment of the proton.

The linear accelerator at Orsay had begun operations in 1959, and by the following year there was an active program of both nucleon and nuclear scattering. The emphasis shifted to colliding-beam experiments in later years, but many scattering experiments were done in the intermediate energy stations of that accelerator with beams of up to 750 MeV.

Electrons had become a big success in high-energy physics, and a new high-energy electron synchrotron was approved and built at Harvard. The Cambridge Electron Accelerator was built jointly by Harvard and MIT and came into operation in 1962 with a peak energy of 5 GeV. A program of electron scattering experiments using internal targets was soon in operation. The new accelerator opened up a new range of  $Q^2$  for scattering experiments, and several different experimental setups were used to measure the proton and neutron form factors. The higher  $Q^2$  proton measurements fell very close to values expected from a straightforward extrapolation of the data at lower energies. The results (Dunning *et al.*, 1964; see also Berkelman *et al.*, 1963) were summed up (somewhat later) by Richard Wilson in the words "The peach has no pit." These results were the first evidence that the old core model of the proton was unlikely to be correct (Fig. 25).

<sup>2</sup>Presented by R. Hofstadter.

## CORNELL ELECTRON SCATTERING SETUP, CIRCA 1960

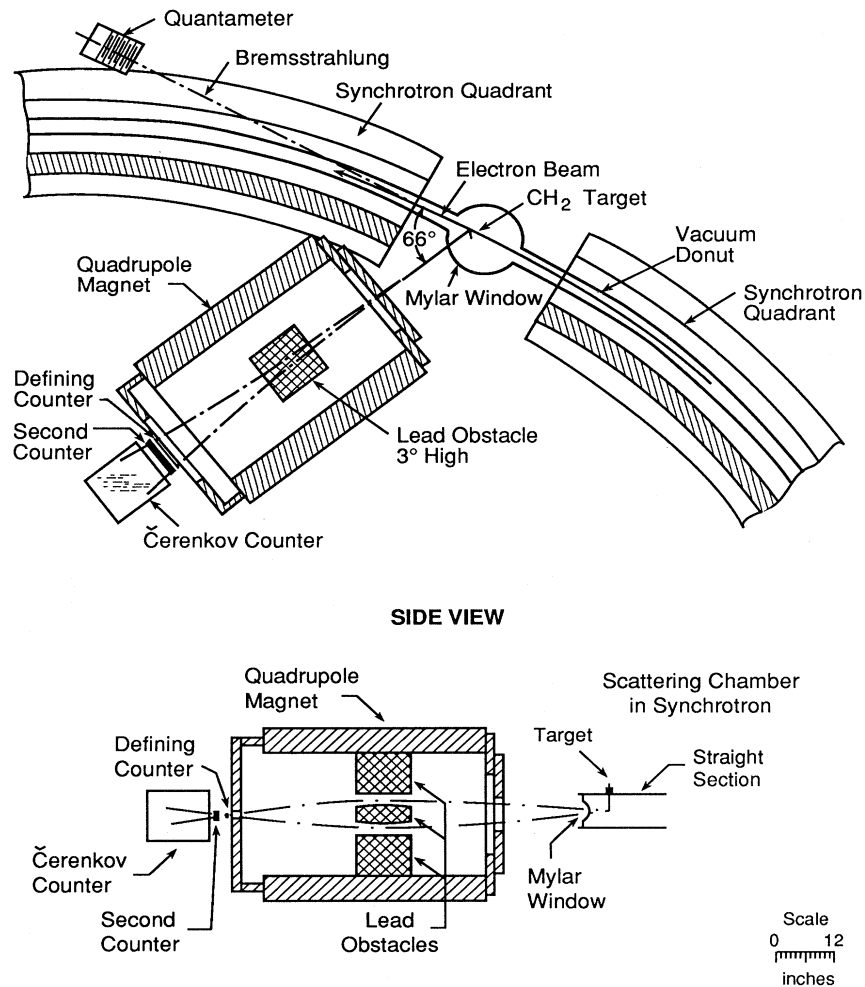


FIG. 24. Schematic of the equipment for electron scattering experiments at Cornell around 1960. These experiments used a quadrupole spectrometer to analyze electrons scattered from an internal target in the electron synchrotron. The target is mounted away from the normal orbit in the accelerator, and the beam is slowly moved onto the target after acceleration.

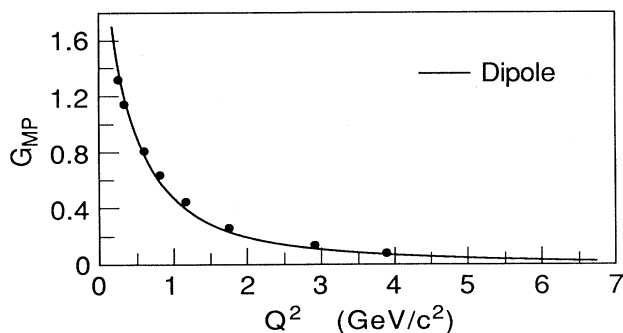


FIG. 25.  $G_M$  for the proton from data taken at CEA. The curve labeled "dipole" is a fit which originated in the late 1950's when the maximum measured  $Q^2$  was limited to less than 1  $\text{GeV}^2$ . It has the form  $G_M = \mu_p / (1 + Q^2 / 0.71 \text{ GeV}^2)^2$  and is in qualitative agreement with the CEA data at higher  $Q^2$ , though the fit is not very good in the statistical sense.

A slightly larger synchrotron was built in Hamburg, Germany at about the same time. DESY came into operation in 1964 with a peak energy of 6 GeV. An extensive series of nucleon scattering measurements using both internal targets (Behrend *et al.*, 1967 and Fig. 26) and external beams (Bartel *et al.*, 1966 and Fig. 27) was undertaken.

With both CEA and DESY operating, the amount of elastic scattering data at high  $Q^2$  (which essentially measures  $G_M$ ) increased rapidly in both quantity and accuracy. The data continued to follow the so-called dipole model to a good approximation. By the Hamburg conference in 1965 there were no dissenters from the view that

$$G_{Ep} = \frac{G_{Mp}}{\mu_p} = \frac{G_{Mn}}{\mu_n},$$

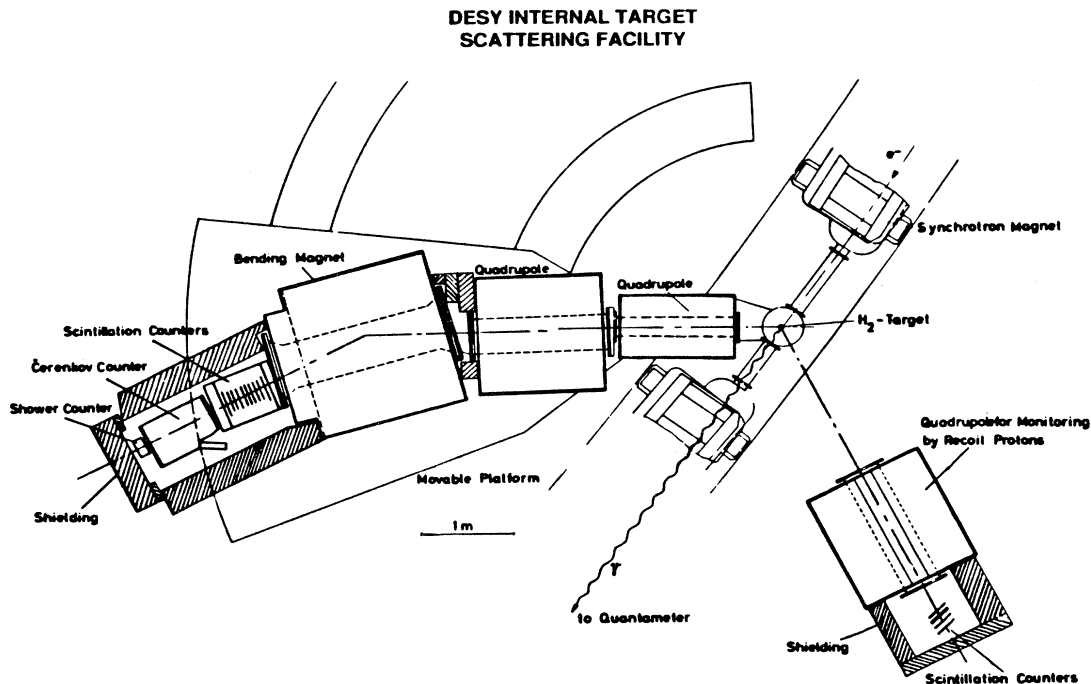


FIG. 26. Layout of the spectrometer setup for internal target electron scattering experiments at DESY. Later on, the same setup was used to detect electron-proton coincidences in elastic scattering (in order to reduce backgrounds).

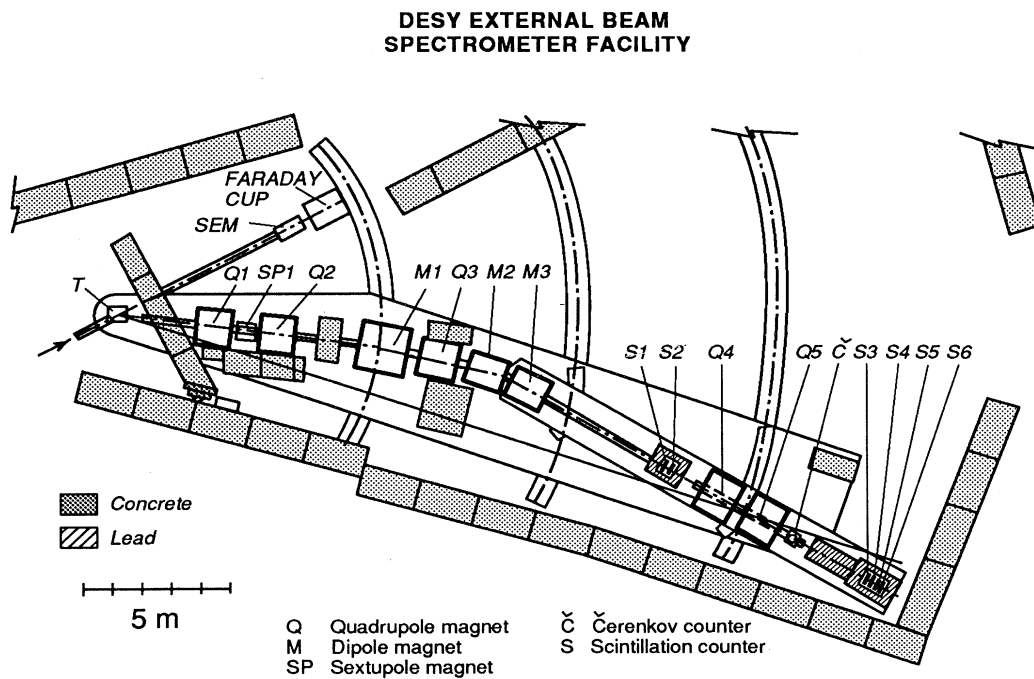


FIG. 27. Setup for external beam scattering experiments at DESY. The spectrometer was articulated between the magnets  $M_2$  and  $M_3$ . By varying the bending in  $M_2$  and  $M_3$ , lines of constant "missing mass" could be adjusted to a given slope at  $S_1$  for different scattered energies.



$$G_{En} \cong 0 \text{ at large } Q^2,$$

and

$$G_{Ep}(Q^2) \cong \left[ \frac{1}{1 + \frac{Q^2}{0.71 \text{ GeV}^2}} \right]^2 \text{ up to } Q^2 \sim 10 \text{ GeV}^2.$$

SLAC was expected to test this formulation in the new range of  $Q^2$  (Fig. 28) made available with 20 GeV electrons. Questions of interest concerned the evidence for a nucleon core and the validity of the dipole description of the form factor in the extended range of  $Q^2$  available at the new accelerator. The cherished picture of a “real proton” surrounded by a meson cloud was already in pretty serious trouble, but more tests for a small core were outlined in the SLAC proposal. Other questions were related to particular models of behavior for the form factors which are not of great interest today.

Our SLAC proposal demanded certain specifications for the beams to be used in the experiment which were within the design specifications of SLAC but which were nonetheless very difficult to meet, given the fact that the accelerator was just being commissioned. Operating the accelerator for the initial scattering experiments was a challenging experience for the crew of accelerator operators, and many of them have indelible memories of those times.

The proposed experiment on elastic scattering aimed at measurements of the cross section at momentum transfers of 16  $\text{GeV}^2$  and beyond, even in the very first

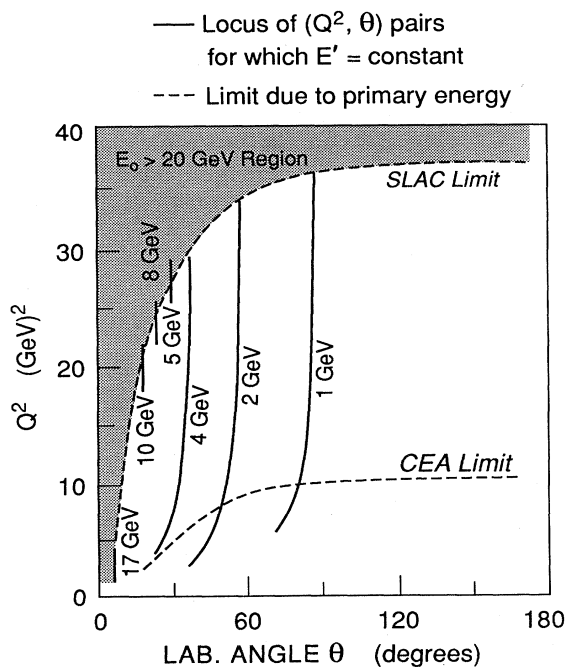


FIG. 28. Plot of elastic kinematics showing the extra kinematic region made available at SLAC for spectrometers of different maximum energies (above 4 GeV, only the maximum  $Q^2$  is indicated to avoid confusion on the graph).

round of experimentation. There was an extensive discussion in the proposal about running at angles and energies in a manner which would result in an efficient separation of  $G_E$  and  $G_M$ . Possible backgrounds were considered, and it was expected that they would be negligible. Radiative corrections to elastic scattering were expected to reach up to 30% for our apparatus and incoming energies of 20 GeV. These corrections arose from two related but physically distinct processes:

(1) Electrons passing through the target and the target windows might emit radiation as a result of interactions with individual atoms (real bremsstrahlung) and thereby suffer an energy loss.

(2) Scattered electrons might emit radiation in the scattering process itself (“wide-angle bremsstrahlung”). The effects of wide-angle bremsstrahlung were first discussed by Schwinger (1949) and have been the subject of increasingly sophisticated calculations over the years.

In some cases the energy of the emitted radiation (in either reaction) was sufficient to affect the kinematics of the scattering to such an extent that the measuring apparatus would no longer “recognize” the interaction. For example, if sufficient (radiative) energy were lost in an elastic scatter, the energy of the scattered electron might fall below the range that the apparatus defined as the “elastic peak.”

The emission of radiation gives rise to the characteristic “radiative tail” in the energy spectrum of elastically scattered electrons as shown schematically in Fig. 29. The cross section measured by detecting the electrons in a certain energy range will be smaller than expected because some particles will be lost. It is customary to correct experimental cross sections for these losses—removing the dependence of the final cross section on the

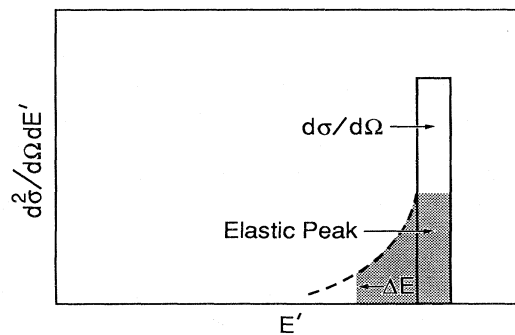


FIG. 29. Radiative effects in elastic scattering. In the absence of radiative effects, all elastic scatters would be found in the box labeled  $d\sigma/d\Omega$  (the width of which depends on resolution in the incoming beam and the detection apparatus). Radiative processes result in energy losses for some scattered electrons, and so some electrons will be found in a “tail” on the low-energy side of the peak. A measurement of the electrons in the shaded region results in a cross section which is somewhat smaller than  $d\sigma/d\Omega$ . This smaller  $(d\sigma/d\Omega)_{\text{meas}}$  can be corrected for radiative losses to determine  $d\sigma/d\Omega$ .

energy resolution of the apparatus.

A simple (first order) correction formula illustrates how such a correction might be applied.

$$\left. \frac{d\sigma}{d\Omega} \right|_{\text{exp}} = (1 - \delta_s) e^{-\delta_r} \frac{d\sigma}{d\Omega}$$

where the wide-angle bremsstrahlung correction  $\delta_s$  is

$$\delta_s = \frac{2\alpha}{\pi} \left\{ \left[ 1 - \ln \frac{Q^2}{m_e^2} \right] \ln \frac{\Delta E}{E} \right\};$$

$m_e$  = mass of the electron ,

$\Delta E$  = energy resolution or acceptance ,

$E$  = incident energy (assumes  $E_s \sim E$ ) ,

and the real bremsstrahlung correction  $\delta_r$  is

$$\delta_r = - \frac{t}{\ln 2} \ln \frac{\Delta E}{E};$$

$t$  = thickness of target in radiation lengths .

As long as the corrections can be calculated to sufficient accuracy, they are innocuous in elastic scattering, and determination of elastic form factors is straightforward.

Our proposal included a possible run plan for measuring  $G_E$  and  $G_M$  to values of  $Q^2$  exceeding 15 GeV<sup>2</sup>. (At the higher  $Q^2$ , one finds an upper bound on  $G_E$ , rather than a measure of its value.) The program was expected to take about 350 hours of beam time, and a first run of 200 hours was suggested, after which the requests would be updated using measured quantities rather than estimates. This experiment was the first to be carried out with the new facility.

The second part of the proposal concerned the measurement of inelastic scattering from the proton. Inelastic scattering from the nucleon had a much shorter history than elastic scattering; so there was much less guidance for the design of that part of our proposal.

Inelastic scattering from *nuclei* was a common feature of the early scattering data at HEPL. The excitation of nuclear levels and the quasi-elastic scattering from the constituent protons and neutrons of a nucleus were observed in the earliest experiments. The excitation of nuclear levels in carbon could be seen in the data of Fig. 4, for example. Quasi-elastic scattering became more evident as momentum transfer was increased. Figure 30 shows scattering from the same target as in Fig. 4, and at approximately the same incident energy, but at a scattering angle of 135°. A comparison of the two figures illustrates the growth in the fraction of quasi-elastic scattering as the angle (and therefore the momentum transfer) is increased. When the electrons scatter through 135°, the elastic peak is very small and the pattern of level excitation has changed because the different multipole transi-

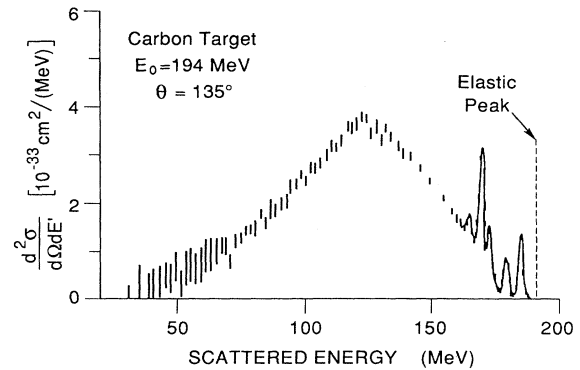


FIG. 30. Spectrum of electrons scattered inelastically from carbon. The excitation of nuclear levels is evident. The large, broad peak between 100 and 150 MeV is due to quasi-elastic scattering from the individual neutrons and protons that make up the carbon nucleus.

tions have different angular dependences. The most prominent feature of the spectrum is the broad quasi-elastic peak in Fig. 30 due to scattering from individual protons and neutrons. The width of the peak reflects the Fermi momentum of the nucleons in the nucleus.

The earliest experiments on the inelastic scattering of electrons from the proton itself were carried out by Panofsky and co-workers at HEPL in the second half of the 1950s (Panofsky *et al.*, 1955, 1956; Yodh and Panofsky, 1957). The early experiments were comparisons of photo- and electroproduction of positive pions in lithium and (later) hydrogen targets. Those experiments checked the calculation of the electromagnetic fields that accompany a relativistic electron, but added little to the knowledge of meson dynamics beyond that which was known from photoproduction (because the dominant contribution to the electroproduction came from virtual photons with very small values of  $Q^2$ ). The authors

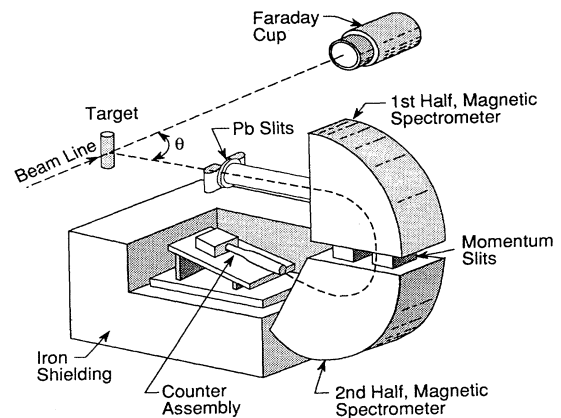


FIG. 31. The zero dispersion magnetic spectrometer used in inelastic experiments at HEPL. Splitting the magnet allowed the insertion of momentum defining slits in the middle of the bend.

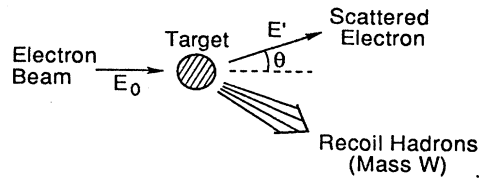
pointed out that observing the scattered *electrons* at large angles (rather than the pions) might lead to more interesting results, and the next experiment was of that kind.

A new magnetic spectrometer was commissioned at HEPL at about this time (Alvarez *et al.*, 1960) and was used for these experiments (Fig. 31). Panofsky and Allton (1958) made measurements of the inelastic scattering of electrons from hydrogen in the region near the threshold for pion production. The energy of the available electrons was not high enough to reach much beyond the threshold for pion production, but the experiment established that the “tail” of the elastic peak was due to the two (calculable) radiative processes mentioned above. One process was elastic scattering preceded (or followed) by emission of bremsstrahlung in the material of the target; the other was “wide-angle bremsstrahlung”—the emission of a photon in the scattering interaction. The experiment was a quantitative test of calculations of the radiative tail of the elastic peak in the region near pion threshold.

The peak energy of the electrons from the Mark III accelerator was improving steadily during those years, and in 1959 Ohlsen (1960) used the 36-inch spectrometer in the Hofstadter group’s scattering facility (Fig. 6) to do an experiment similar to the Panofsky-Allton measurement. With increased energy, it was possible to make measurements covering the region of the first  $\pi$ - $p$  resonance, and a clear peak was observed at the resonance energy. The

experimenters were also able to measure a rough  $Q^2$  dependence of the peak cross section.

In 1962, Hand reported on a similar experiment (using the same spectrometer used by Allton) and the results were discussed in modern notation. In particular, there appears an inelastic equivalent of the Rosenbluth formula containing two form factors which are functions of  $Q^2$  and  $\nu$ , the energy loss suffered by the scattered electron. The measured quantities are  $E_0$ ,  $E'$ , and  $\theta$ :



The kinematics of the scattering are described by

$$E' = \frac{E_0 - \frac{(W^2 - M^2)}{2M}}{1 + \frac{2E_0}{M} \sin^2 \theta / 2}$$

$W$  is the mass of the final state of the struck hadron (when  $W^2 = M^2$ , the elastic kinematics are recovered). The square of the momentum transfer,  $Q^2$

$$Q^2 = 4E_0 E' \sin^2 \theta / 2,$$

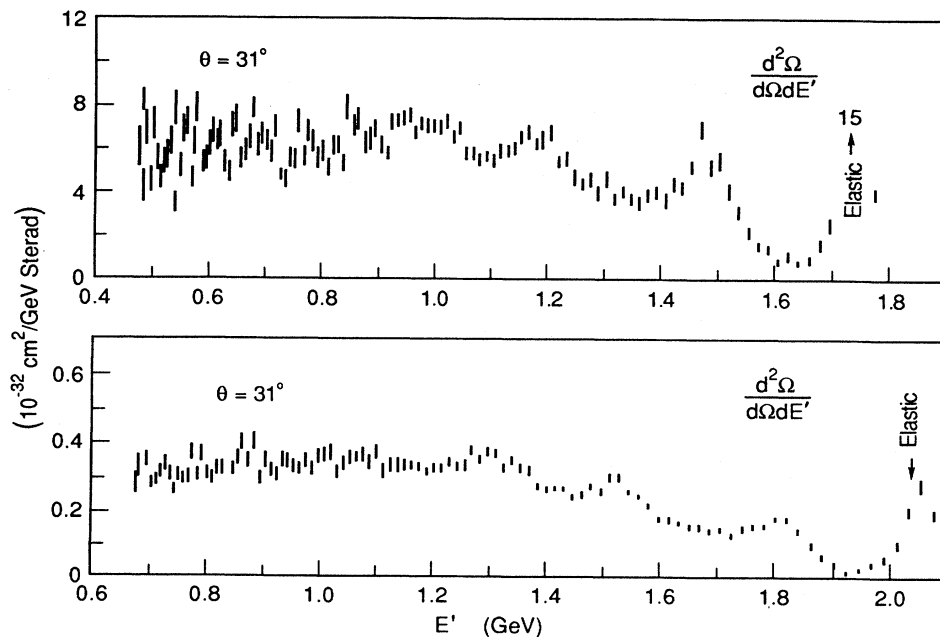


FIG. 32. Inelastic spectra from CEA at  $31^\circ$  for initial energies of 2.4 GeV and 3.0 GeV. Three bumps are clearly evident corresponding to resonance excitations of the proton.

the energy loss

$$\nu = E_0 - E',$$

and  $W^2$  are relativistically invariant quantities in the scattering process.

There are two equivalent formulations describing the cross sections which are in current use. One, due to Drell and Walecka (1964), is very similar in form to the Rosenbluth expression,

$$\frac{d\sigma}{d\Omega dE'} = \frac{\alpha^2}{4E_0^2 \sin^2 \theta/2} \cos^2(\theta/2) [W_2 + 2W_1 \tan^2 \theta/2].$$

The structure functions  $W_1$  and  $W_2$  are functions of both the momentum transfer and energy loss,  $W_{1,2}(Q^2, \nu)$ . This is the most general form of the cross section in the (parity conserving) one photon approximation.

Hand (1963) popularized a different but equivalent form for the cross section in which one of the form factors reduces to the photo-production cross section at  $Q^2=0$ ,

$$\frac{d\sigma}{d\Omega dE'} = \frac{\alpha^2}{4\pi^2} \frac{(W^2 - M^2)E'}{MQ^2 E_0(1-\epsilon)} (\sigma_T + \epsilon\sigma_L)$$

where

$$\epsilon = \frac{1}{1 + 2 \tan^2(\theta/2)(1 + \nu^2/Q^2)}.$$

Again,  $\sigma_T$  and  $\sigma_L$  (corresponding to the photo cross sections for transversely polarized and longitudinally polarized virtual photons, respectively) are functions of the momentum transfer and energy loss of the scattered electron,  $\sigma_{L,T}(Q^2, \nu)$ , with the limiting values at  $Q^2=0$  of

$$\sigma_T(0) = \sigma_{\gamma p}, \quad \sigma_L(0) = 0.$$

These early experiments and the associated theoretical studies developed much of the framework for thinking about inelastic experiments at SLAC. The energy available limited the early experiments on the proton to studies of the  $\pi$ - $p$  resonance near 1238 MeV.

An important influence came from the Laboratoire de l'Accelérateur linéaire in Orsay, where experiments on inelastic electron scattering from nuclei led to the study of radiative processes, and to the determination of radiatively corrected cross sections from inelastic scattering data.

The focus of our thinking about inelastic experiments during the construction period centered on the excitation of resonances and the  $Q^2$  dependences of the "transition form factors" (the nucleon makes a transition from the ground state to the resonant state). We hoped to learn more about each of the observable resonances, and also expected to see new resonances that had not been electro-produced before and even some that had never been observed before in any reaction. Just before the proposal was submitted, data from the CEA were published (Cone *et al.*, 1965) showing clear evidence of three

resonant states excited by inelastic electron scattering. The group at CEA used a quadrupole spectrometer to obtain spectra like those in Fig. 32. The background of radiative events is substantial. Very interesting spectra from DESY (Brasse *et al.*, 1968) showing large non-resonant contributions to the inelastic cross section would come later, at about the time that the first (inelastic) experiments were starting up at SLAC.

Our proposal was approved in 1966, along with proposals from other groups. The running time for the various parts of our proposal was interleaved with other runs to study photo-production with the spectrometer facility (and with experiments on a streamer chamber which occupied a building behind End Station A and which used the same beam line).

By January of 1967, the 8 GeV spectrometer was nearly complete and we were beginning preparations for the

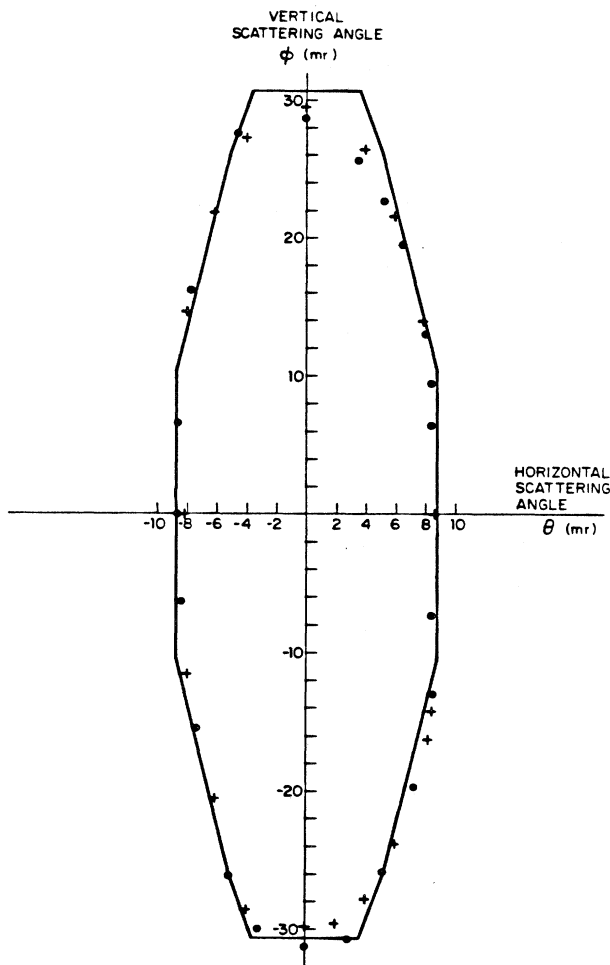


FIG. 33. Angular acceptance of the 8 GeV spectrometer for electrons from the center of the target and with the spectrometer set so that the incoming beam followed the central axis. The points are for two different beam energies ( $\bullet$ =8 GeV,  $+$ =6 GeV). The solid line is the aperture from computer calculations.

initial elastic scattering experiment.

The solid angle of the spectrometers entered directly into the calculation of the cross section, and we wanted to check the calculations of the 8 GeV aperture. A special run with beam was planned to study the optics of the spectrometer and the acceptance. The spectrometer was placed at  $0^\circ$  so that the beam entered the spectrometer along the central orbit. The beam energy was adjusted to the setting of the spectrometer, and the beam was observed with scintillation screens mounted at the focal planes. Magnets located at the target position steered the beam, tracing out orbits and verifying the optical properties of the spectrometer's magnetic fields. By determining the limiting orbits in the spectrometer, the solid angle could be measured. Figure 33 shows the results for the central momentum case. The agreement with the predictions was quite good, but there were some slight discrepancies with the calculated aperture limits for the extreme rays. After the initial run, lead masks were introduced into the spectrometer to better define the aperture.

Following the optics tests, the counters and shielding were installed along with the hydrogen target and the beam current monitors. By the month of May the first runs of the elastic scattering experiment were underway. The accelerator was operating rather well by this time, though still struggling to meet all of the design specifications.

It is an exciting moment when a new experimental facility is put into operation at a new accelerator, especially

when the new accelerator opens up extended new regions of energy for exploration. We were about to use the biggest physics project ever built to look into places where no one had ever looked before. Nearly a decade of thinking and hard work by hundreds of people would be tested by the events of that evening. Such moments are often spoiled by last-minute difficulties, but we were fortunate. Preparations proceeded smoothly, the target was filled with hydrogen, and soon the computer was analyzing events. Within a few minutes a respectable elastic peak was showing in the " $p$ - $\theta$ " display which sorted events into bins corresponding to the counters hit in the momentum and scattering angle hodoscopes (Fig. 34). The data in this 3-dimensional plot can be converted to a 2-dimensional plot of counts versus missing mass (Fig. 35) and then to cross sections and form factors. For the next couple of weeks we accumulated data and ran various checks. The system worked well—we could accumulate data fairly rapidly and change both energy and angle from the counting house. The investments made for the sake of efficiency were proving to be valuable, and we were happy with the functioning of our apparatus and the operation of the accelerator.

A preliminary analysis of the data obtained was made within a few months for presentation at the Electron-Photon Symposium held in SLAC in August 1967 (Taylor, 1967). The elastic cross sections measured at SLAC behaved in much the same way as those measured at lower energies—falling on the same simple extrapolation of the earlier fits as the CEA and DESY data (Fig. 36).

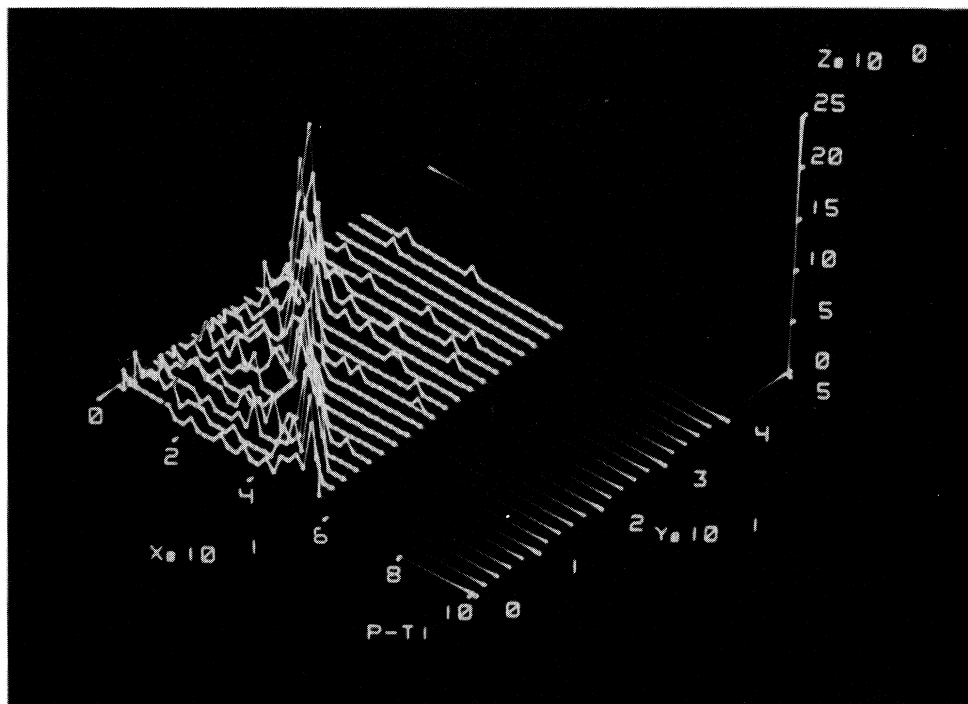


FIG. 34. Computer display of the focal plane location of particles passing through the elements of the  $p$  and theta hodoscopes of the 8 GeV spectrometer. The line corresponding to elastic scattering is evident.

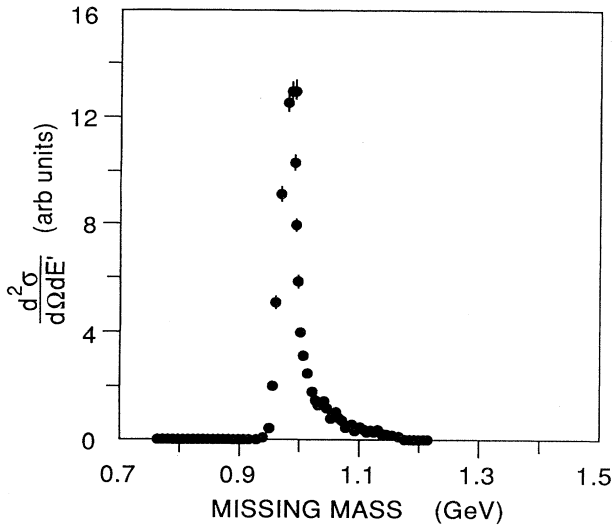


FIG. 35. The same data as in Fig. 34, plotted against the calculated missing mass of each event. (The peak is displaced from the mass of the proton at 938 MeV by a slight mismatch in energy calibrations between the switchyard and the spectrometer.)

We collected data for  $G_M$  at values of  $Q^2$  up to  $25 \text{ GeV}^2$ .

The first opportunity to find something new and unexpected with the spectrometer facility and the SLAC beam had been a disappointment. This is quite normal in experimental physics. Most measurements increment knowledge by just a small amount. Sometimes enough of those small increments eventually results in insights that change our point of view. The sudden observation of unexpected phenomena that result in major new insights is an uncommon event in science. One tries to be ready for such observations, but usually has to be content with adding a small brick of knowledge to the existing edifice. In any case, we had very little time to philosophize over the elastic results because we were busy preparing for the first inelastic scattering experiments. They began in August 1967, using the 20 GeV spectrometer.

In this talk I have tried to point out the importance of advances in accelerators and experimental equipment for the long series of electron scattering experiments at Stanford and elsewhere. The utility of large-scale facilities would continue to be demonstrated in later work on nuclear structure with muons and neutrinos at Fermilab and CERN. Large facilities are now commonplace in high-energy physics, partly because of the early successes of such facilities in the field of electron scattering.

The Stanford Linear Accelerator and the associated initial complement of experimental equipment were generously supported by U.S. Government funding administered by (what is now) the Department of Energy. We were given a chance to build apparatus that was well suited to the opportunities provided by the new linear accelerator. The vast changes in the scale of scientific endeavors during this century have not changed one of the principal preoccupations of the experimental physicist—

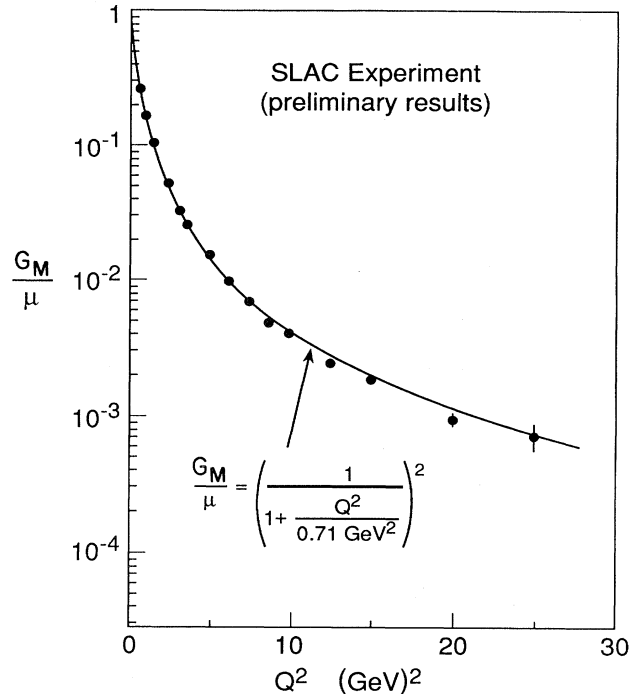


FIG. 36. Magnetic form-factor measurement at SLAC in 1967. The dipole curve is the same as in Fig. 25, here extended to  $Q^2 = 25 \text{ GeV}^2$ . Again, the agreement is imperfect, but the curve describes the general behavior of the data quite well.

the building of quality experimental equipment which is matched to the task at hand. In those days the cost-effectiveness of apparatus was considered more important than arbitrary cost ceilings, and we hope that the physics output of the facilities in End Station A has justified the considerable expense incurred in building them.

In the summer of 1967, SLAC was embarking on a long and productive program of experiments. The story of one of those experiments will be continued in Professor Kendall's lecture.

## REFERENCES

- Alvarez, R. A., K. L. Brown, W. K. H. Panofsky, and C. T. Rockhold, 1960, *Rev. Sci. Instrum.* **31**, 556.
- Bartel, W., B. Dudelzak, H. Krehbiel, J. M. McElroy, U. Meyer-Berkhout, R. J. Morrison, H. Nguyen-Ngoc, W. Schmidt, and G. Weber, 1966, *Phys. Rev. Lett.* **17**, 608.
- Behrend, H. J., F. W. Brasse, J. Engler, H. Hultschig, S. Galster, G. Hartwig, H. Schopper, and E. Ganssauge, 1967, *Nuovo Cimento A* **48**, 140.
- Berkelman, K., M. Feldman, R. M. Littauer, G. Rouse, and R. R. Wilson, 1963, *Phys. Rev.* **130**, 2061.
- Brasse, F. W., J. Engler, E. Ganssauge, and M. Schweizer, 1968, *Nuovo Cimento A* **55**, 679.
- Buchanan, C. D., *et al.*, 1965, in *Electron and Photon Interactions at High Energies*, Proceedings of the International Symposium held in Hamburg, Germany, 1965, Springer Tracts in Modern Physics Vol. 39, edited by G. Höhler (Springer-

- Verlag, Berlin/Heidelberg), pp. 20–42.
- Cone, A. A., K. W. Chen, J. R. Dunning, Jr., C. Hartwig, N. F. Ramsey, J. K. Walker, and Richard Wilson, 1965, *Phys. Rev. Lett.* **14**, 326.
- Drell, S. D., and J. D. Walecka, 1964, *Ann. Phys. (NY)* **28**, 18.
- Dunning, J. R., Jr., K. W. Chen, A. A. Cone, G. Hartwig, and Norman F. Ramsey, 1964, *Phys. Rev. Lett.* **13**, 631.
- Franck, J., and G. Hertz, 1914, *Verh. Dtsch. Phys. Ges.* **16**, 457.
- Fregeau, J. H., and R. Hofstadter, 1955, *Phys. Rev.* **99**, 1503.
- Friedman, J. I., 1991, “Deep inelastic scattering: comparisons with the quark model,” Nobel Lecture, in *Les Prix Nobel 1990: Nobel Prizes, Presentations, Biographies and Lectures* (Almqvist & Wiksell, Stockholm/Uppsala), in press; reprinted in *Rev. Mod. Phys.* **63**, 615.
- Friedman, J. I., H. W. Kendall, and R. E. Taylor, 1991, Nobel Lecture Acknowledgments, in *Les Prix Nobel 1990: Nobel Prizes, Presentations, Biographies and Lectures* (Almqvist & Wiksell, Stockholm/Uppsala), in press; reprinted in *Rev. Mod. Phys.* **63**, 629.
- Geiger, H., and E. Marsden, 1909, *Proc. R. Soc. London* **82**, 495.
- Ginzton, E. L., *et al.*, 1957, Proposal for a two-mile linear electron accelerator at Stanford University, submitted April 1957, unpublished.
- Hand, L., 1963, *Phys. Rev.* **129**, 1584.
- Hofstadter, R., 1956, *Rev. Mod. Phys.* **28**, 214.
- Hofstadter, R., and R. W. McAllister, 1955, *Phys. Rev.* **98**, 217.
- Kendall, H. W., 1991, “Deep inelastic scattering: experiments on the proton and the observation of scaling,” Nobel lecture, in *Les Prix Nobel 1990: Nobel Prizes, Presentations, Biographies and Lectures* (Almqvist & Wiksell, Stockholm/Uppsala), in press; reprinted in *Rev. Mod. Phys.* **63**, 597.
- Lyman, E. M., A. O. Hanson, and M. B. Scott, 1951, *Phys. Rev.* **84**, 626.
- Neal, R. B., 1968, Ed., *The Stanford Two-Mile Accelerator* (Benjamin, New York).
- Ohlsen, G. G., 1960, *Phys. Rev.* **120**, 584.
- Panofsky, W. K. H., and E. A. Allton, 1958, *Phys. Rev.* **110**, 1155.
- Panofsky, W. K. H., C. Newton, and G. B. Yodh, 1955, *Phys. Rev.* **98**, 751.
- Panofsky, W. K. H., W. M. Woodward, and G. B. Yodh, 1956, *Phys. Rev.* **102**, 1392.
- Rose, M. E., 1948, *Phys. Rev.* **73**, 279.
- Rosenbluth, M. N., 1950, *Phys. Rev.* **79**, 615.
- Rutherford, E., 1911, *Philos. Mag.* **21**, 669.
- Schiff, L. I., 1949, *Summary of Possible Experiments with a High Energy Linear Electron Accelerator*, SUML-102 (Stanford University, Microwave Laboratory), unpublished.
- Schwinger, J., 1949, *Phys. Rev.* **75**, 898.
- Taylor, R. E., 1967, in *Proceedings of the 1967 International Symposium on Electron and Photon Interactions at High Energies*, Stanford Linear Accelerator Center, September 1967 (SLAC, Stanford), pp. 78–101.
- Wilson, R. R., 1957, *Nucl. Instrum.* **1**, 101.
- Wilson, R. R., K. Berkelman, J. M. Cassels, and D. N. Olson, 1960, *Nature* **188**, 94.
- Yodh, G. B., and W. K. H. Panofsky, 1957, *Phys. Rev.* **105**, 731.

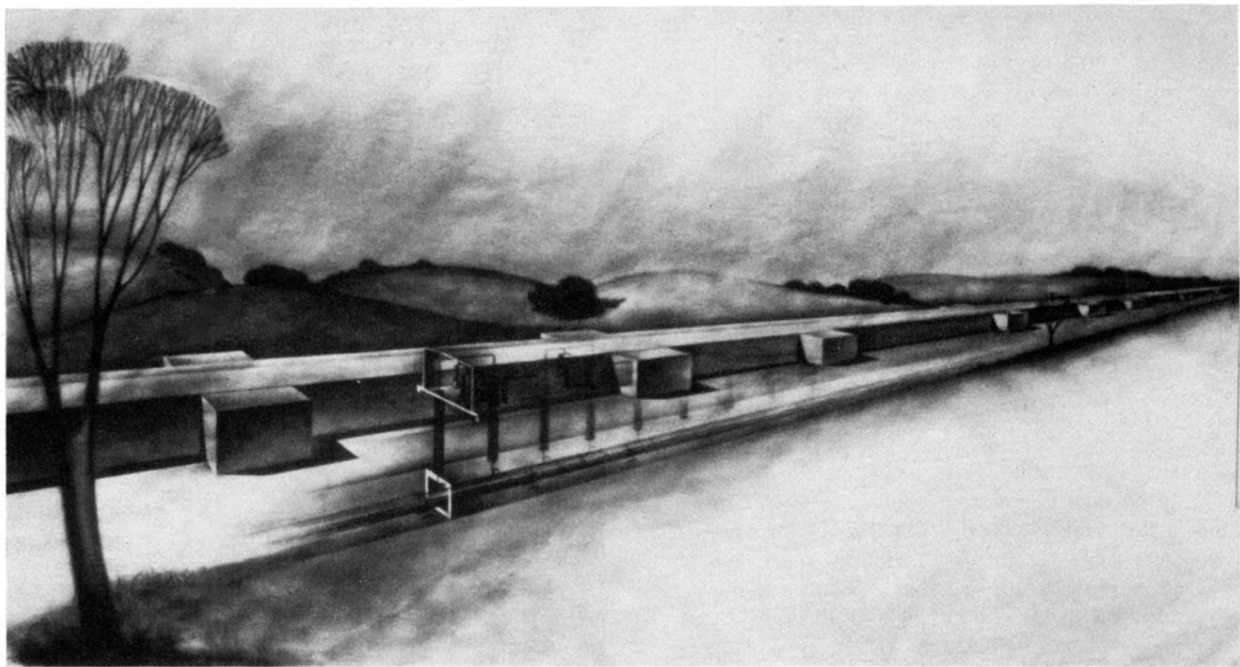


FIG. 10. Cutaway illustration of the two-mile Stanford Linear Accelerator, showing the accelerator waveguide buried 25 feet below the surface and the klystron gallery at ground level. Each klystron feeds 40 feet of accelerator waveguide through penetrations connecting the accelerator housing with the klystron gallery.



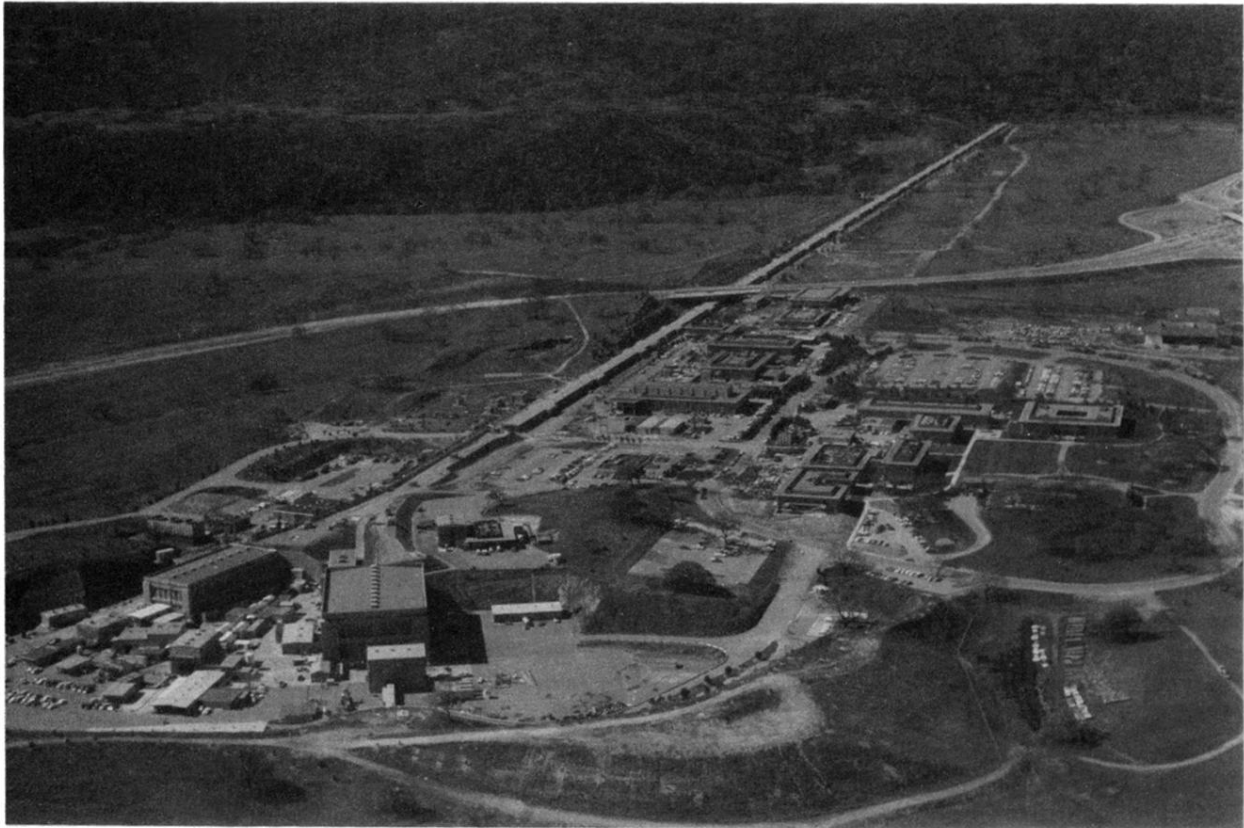


FIG. 11. Aerial view of the SLAC site. On the left are the experimental areas fed by beam lines from the accelerator. On the right is the campus area where offices, laboratories, and shops are located. The scattering experiments were performed in the large shielded building just to the left of center near the bottom of the picture. The structure crossing the accelerator is a superhighway which was under construction at the time this picture was taken.

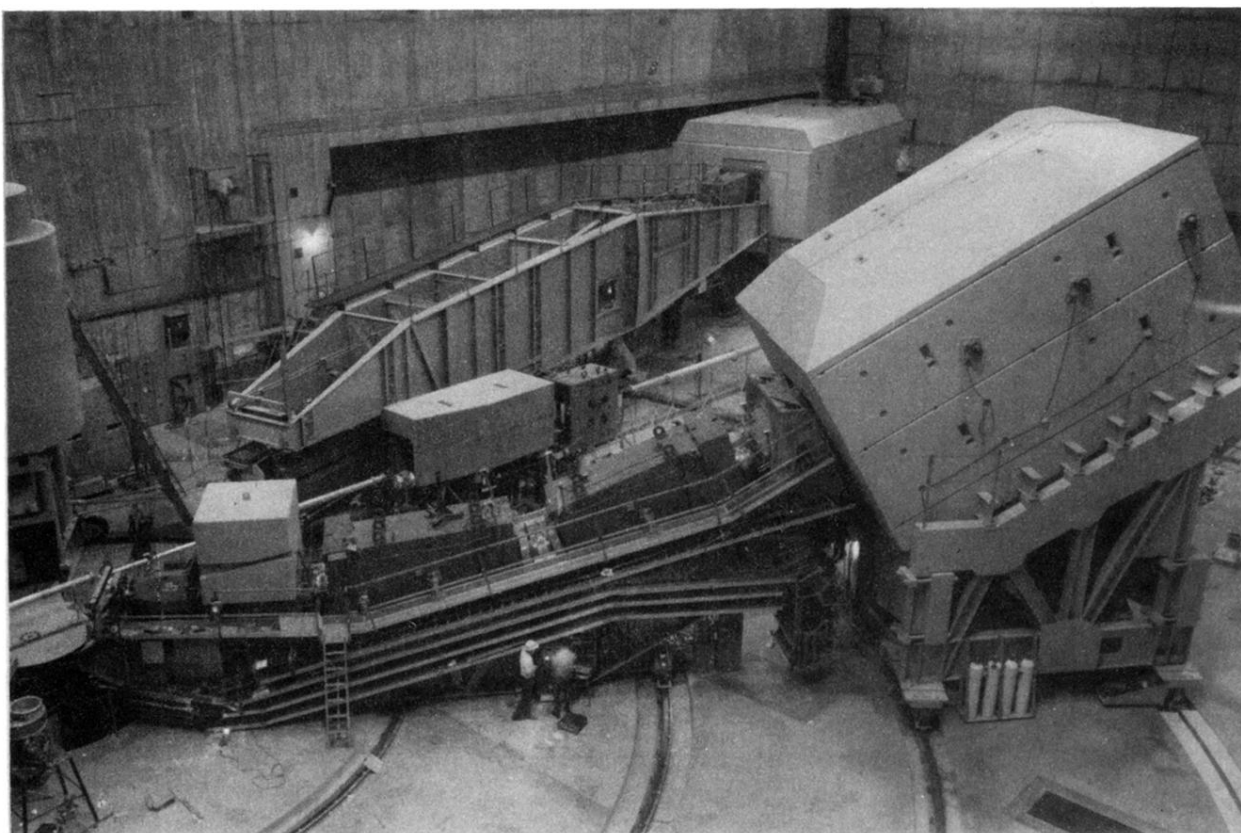


FIG. 20. Photograph of the 8 and 20 GeV spectrometers in End Station A.

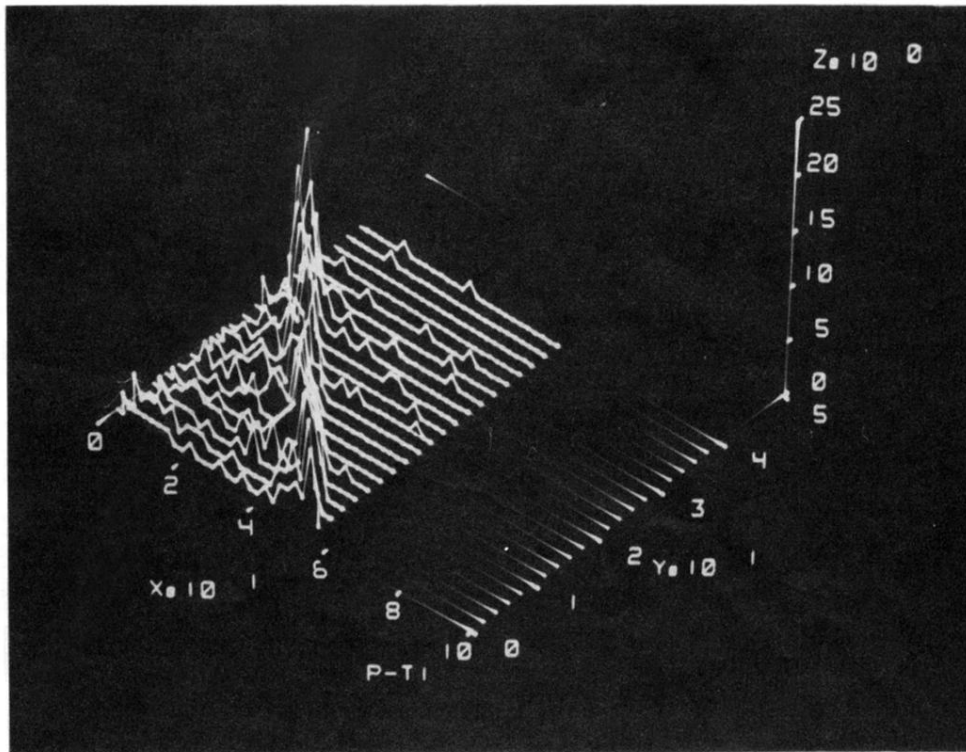


FIG. 34. Computer display of the focal plane location of particles passing through the elements of the  $p$  and theta hodoscopes of the 8 GeV spectrometer. The line corresponding to elastic scattering is evident.